POSTER PRESENTATIONS

PO1
OCTREOTIDE OR DOTATATE. IS THERE A DIFFERENCE?

S Johnson[1], D Bailey[1]

[1]Guys and St Thomas Hospital, London, UK

Background: Department protocol for patients undergoing Peptide Receptor Radionuclide Therapy (PRRT) is an initial pre-treatment feasibility scan, followed by post-treatment response scans at three month intervals for a year and then six monthly surveillance scans. Ideally all scans should be imaged with In-111 Dotatate however due to availability, patients were administered In-111-Octreotide for follow up scans as a substitute for In111 Dotatate.

Aim: Identify any scan differences in patients that have had In-111 Octreotide and In-111 Dotatate follow up imaging.

Methods: Visually assess Nuclear Medicine imaging performed during treatment of PRRT. This includes pre-treatment, therapy and follow up scans. Identify any changes to tumour response.

Discussion and Results: In a 9 month period three patients were administered with In111-Octreotide for follow up scans after Lu-177 Dotatate therapy. It was noted in these scans that there was reduced tumour uptake compared to previous imaging. The doctors not knowing whether this was due to disease progression monitored patients by blood tests and follow up In-111 Dotatate scan. Patient's current In-111 Dotatate demonstrated stable disease uptake comparable to previous Dotatate imaging.

Conclusion: In-111 Dotatate is the preferred radioisotope for follow up scans for PRRT patients.

PO2
MANAGEMENT IMPACT OF VESICULAR MONOAMINE TRANSPORTER (VMAT) IMAGING WITH [18F]AV133 IN CLINICALLY UNCERTAIN PARKINSONIAN SYNDROMES (CUPS)

C Sivaratnam[1], S Pejoska[1], Y Lie[1], V Villemagne[1,2], G Jones[1], R Mulligan[1], S Chowdry[1], F Iftikhar[1], K Young[1], S Jesudason[1], C Rowe[1]

[1]Department of Molecular Imaging and Therapy, Austin Health, Melbourne, Australia
[2]Florey Institute of Neuroscience and Mental Health, University of Melbourne, Melbourne, Australia

Objective: Misdiagnosis of Parkinson's disease initially occurs in up to 30% of patients and in 10–15% after long term follow-up. Dopamine transporter (DAT) SPECT has been shown to change diagnosis in up to 50% of clinically uncertain Parkinsonian syndromes (CUPS). VMAT-II PET imaging with the tetrabenazine derivative, [18F]AV133, provides high quality images of striatal dopaminergic synaptic density with shorter uptake and imaging times than DAT SPECT. We therefore examined the management impact of [18F]AV-133 PET in CUPS.

Methods: 47 patients with CUPS were recruited from movement disorder specialists who completed diagnosis and management questionnaires pre- and post-release of the PET findings. Imaging was acquired for 20 minutes, 2 hours post-injection of 250 MBq of [18F]AV133. Images were read visually and quantitatively as ratio of caudate, anterior and posterior putamen to occipital cortex. Change in diagnosis, medication and diagnostic confidence was recorded and rated as nil, low (confirmation of diagnosis), moderate (alteration in management) or high (change in diagnostic class i.e. neurodegenerative PD to other or vice versa).

Results: A change in diagnostic class occurred in 14 (30%). Medication change occurred in another 14 (30%). Overall, management impact was rated as moderate or high in 60% of subjects. High clinician diagnostic confidence increased from 3 patients to 35 post-scan.

Conclusion: [18F]AV133 PET had substantial management impact in patients with clinically uncertain Parkinsonian syndromes, similar to that reported for DAT SPECT, but with the advantage of shorter preparation, uptake and imaging times and the better image quality of PET.

PO3
PROSPECTIVE STUDY OF WHOLE BODY FDG PET/CT IN PATIENTS WITH POLYMYALGIA RHEUMATICA

C Owen[1], A Poon[2], ST Lee[2], K Pathmaraj[2], R Buchanan[1], AM Scott[2]

[1]Department of Rheumatology, Austin Health, Melbourne, Australia
[2]Department of Molecular Imaging & Therapy, Austin Health, Melbourne, Australia

Background: Polymyalgia Rheumatica (PMR) is a common chronic inflammatory disorder characterised by subacute onset shoulder and pelvic girdle pain, and early morning stiffness. In the absence of a gold standard test, diagnosis is based upon clinical features and raised inflammatory markers. Treatment entails a weaning course of prednisolone prescribed in a 'one size fits all' approach, however heterogeneity in the response to standard therapy is observed among patients. Whole body FDG PET/CT possesses the unique ability to evaluate the distribution of active inflammatory disease, which may impact upon the longitudinal outcomes of patients with PMR.

Aim: To characterise the distribution of FDG uptake on whole body PET/CT in patients with newly diagnosed PMR.

Methods: Patients with newly diagnosed PMR according to the American College of Rheumatology (ACR) 2012 Classification Criteria were prospectively recruited. Whole body PET/CT was conducted at baseline and all patients were prednisolone-naïve prior to scanning. Demographic, clinical and laboratory data were also collected. Additional imaging investigations included hand x-rays and ultrasound of the hands, shoulders and hips. A standardised protocol of prednisolone treatment was commenced following enrolment.

Results: Eight patients have satisfied the inclusion criteria thus far. All were Caucasian, aged >50 years, and presented with symptoms of bilateral shoulder and/or hip girdle pain. The pattern of FDG uptake was noted to be principally peri-articular and capsular in distribution, as opposed to intra-articular as seen in patients with osteoarthritis. Principal sites of uptake included bilateral shoulder and hip joint capsules, tendon insertions, and widespread bursa involvement including the interspinous bursae.

Conclusions: The distribution of FDG in patients with PMR is distinct from the intra-articular pattern of uptake in patients with osteoarthritis. The extent and degree of uptake may influence the response to prednisolone therapy, and will be explored as a prognostic indicator in longitudinal studies.

PO4
EMERGING ROLE OF FDG-PET IN THE DIAGNOSIS OF IGG4 RELATED DISEASE: A CASE OF MULTIORGAN INVOLVEMENT

A Iravani[1], R Mansberg[1,2], L Shen[1], B Champion[1,2]

[1]Department of Nuclear Medicine and PET, Nepean Hospital, NSW, Australia
[2]University of Sydney, NSW, Australia

Background: Immunoglobulin G4-related disease (IgG4-RD) is an increasingly recognized syndrome of unknown etiology comprised of a collection of disorders that share specific pathologic, serologic and clinical features, involving almost any organ. Definitive assessments of the incidence and prevalence of IgG4-RD in general population are lacking. Although, elevated serum concentrations of IgG4 are found in 60–70% of patients, they are nonspecific. Diagnosis of IgG4-RD is predominantly based upon biopsy findings; however, recent data suggest FDG-PET can be highly effective in determining the extent of disease and detects significantly more lesions (71.4% of patients) than conventional imaging. FDG-PET is useful in the assessment of the early response to steroid based treatment which will aid to exclude possible concurrent malignancies.

Aims: To demonstrate the role of FDG-PET in the diagnosis, detecting multiorgan involvement and monitoring response to treatment in IgG4-RD.

Methods and Results: We present a 67-year-old male with multiorgan IgG4-RD. Diagnosis was made on the basis of lymph node biopsy, raised IgG4 serum level (16.6 g/L, normal range 0.3–2.0 gr/L) and typical multiorgan involvement on FDG-PET. FDG-PET detected involvement of more organs compared to conventional imaging including CT and MRI. FDG-PET showed diffuse uptake in the pancreas consistent with pancreatitis with no significant abnormality on MRI, in salivary glands with normal appearance on CT. There was also uptake along the biliary tree corresponding to multifocal strictures on MRI, consistent with sclerosing cholangitis, in a

© 2015 The Authors
Internal Medicine Journal © 2015 Royal Australasian College of Physicians

lung nodule, and in axillary, inguinal and hilar lymph nodes. Corticosteroids were commenced with good clinical and laboratory response (IgG4 7.3 gr/L).

Conclusion: FDG-PET is becoming an essential tool in many aspects of IgG4-RD, including diagnosis, targeting interventional biopsy, evaluating multiorgan involvement and monitoring therapeutic response. The imaging pattern, including PET has also been suggested to be updated into the consensus diagnostic criteria for IgG4-RD.

PO5
THE PREVALENCE OF EXTRASKELETAL FINDINGS ON THE UNENHANCED LOW DOSE CT COMPONENT OF THE 18F-FLUORIDE PET/CT BONE SCAN IN BREAST CANCER PATIENTS

R Brown[1], R Menghis Berhane[1], R K Kulshrestha[1,2], S Vinjamuri[1]

[1]Royal Liverpool University Teaching Hospital NHS Trust, Liverpool, UK
[2]Central Manchester University Teaching Hospitals NHS Foundation Trust, Manchester, UK

Background: The low dose CT provides vital 'extra' information other than confirming or excluding bone metastatic disease. It is also very useful for looking at the remaining tissues throughout the neck, thorax, abdomen and pelvis and identifying clinically important and non-important incidental findings.

Aims: To determine the prevalence of incidental extra-osseous findings on the un-enhanced CT component of the 18F-Fluoride PET/CT bone scans, and to then determine their clinical significance.

Methods: Retrospective data analysis of all patients with breast cancer in 2013 that had 18F-Fluoride bone scans with incidental findings. All positron emission tomography (PET) scans were reported by a nuclear medicine physician with the un-enhanced computed tomography (CT) being reviewed by either another experienced physician or radiologist. All incidental CT findings that were subsequently found to be previously known were excluded. A total of 343 18F-Fluoride scans were performed on patients with a history of current or previous breast cancer in 2013.

Results: Of the 343 scans performed, 83 (24%) had incidental findings, with two patients scanned twice within the year, each having separate incidental findings. 22% of incidental findings were in the pelvis. The majority of these did not have a separate CT scan of the pelvis. Of the patients with incidental findings, 52 (63%) were potentially significant. Examples include: foraminal encroachment as a consequence of metastatic vertebral collapse, suspected primary lung cancer, indeterminate lung nodules, adrenal masses, suspicious adnexal masses, pancreatic calcification and omental metastases causing small bowel obstruction.

Conclusion: The incidental findings present a challenge as well as an opportunity to detect previously unknown pathology. Careful evaluation of the low dose CT component of the PET/CT is important since a significant number of patients have coincidental findings, which may alter management and prognosis.

PO6
FOLLOW-UP STUDIES OF 18-F SODIUM FLUORIDE PET/CT BONE STUDIES IN PATIENTS WITH BREAST CANCER BONE METASTASES: PLANAR BONE SCINTIGRAPHY VERSUS 18F-FLUORIDE PET/CT: WHICH ARE WE DOING AND WHY?

R K Kulshrestha[1,2,3], S Vinjamuri[2], P Hogg[3], A England[3]

[1]Central Manchester University Teaching Hospitals NHS Foundation Trust, Manchester, UK
[2]Royal Liverpool University Teaching Hospitals, Liverpool, UK
[3]University of Salford, Salford, UK

Background: No research has concluded on whether it is more beneficial to carry-out bone scintigraphy or 18F-Fluoride PET/CT as a follow-up study in breast cancer patients who have suspected metastatic bone disease. This clearly has dose implications for the patient.

Aims: To investigate a pattern in the selection process for follow-up studies of 18-F Fluoride PET/CT bone studies versus planar bone scintigraphy. To outline any major reasons or patterns found why one study was chosen over the other.

Methods: Retrospective review of 85 known breast cancer patients. To calculate the proportion of patients who had follow-up studies after 18F-Fluoride. To observe any pattern recognition process for a particular test chosen.

Results: 23/85 (27%) patients had follow-up studies performed. 13/23 patients had a positive initial 18-F Fluoride PET/CT study, and received a similar subsequent PET/CT study. 4/23 had a negative 18-F Fluoride PET/CT, and hence had a follow-up bone scan. 3/23 had a negative initial 18-F Fluoride PET/CT, however had a repeat 18-F Fluoride PET/CT bone study due new onset of rib/chest pain. 2/23 had a positive 18F-Fluoride PET/CT and then planar bone scintigraphy as follow-up (no apparent reason given). 1/23 had a false positive 18-F Fluoride PET/CT, and had subsequent planar bone scintigraphy.

Conclusion: Having a positive 18-F Fluoride PET/CT study initially with bone metastases and degenerative changes, tended to require a repeat 18-F-Fluoride PET/CT study to more accurately monitor metastatic bone disease, and to compare 'like with like.' Having a negative 18-F Fluoride study was very reassuring initially and hence was tended to be followed-up with conventional bone scintigraphy, so long as it did not develop bone pain symptoms.

PO7
18F-FLUOROETHYL-TYROSINE PET IN DIFFERENTIATING RECURRENT GLIOMA AND RADIATION NECROSIS: A RETROSPECTIVE SINGLE CENTER STUDY

A Iravani[1], C Bui[1], L Shen[1], A Stevanovic[2], R Mansberg[1,3]

[1]Department of PET and Nuclear Medicine, Nepean Hospital, Kingswood, Australia
[2]Department of Oncology, Nepean Hospital, Kingswood, Australia
[3]University of Sydney, Sydney, Australia

Background: Amino acid PET tracers such as fluoroethyl-tyrosine (FET) offer powerful molecular imaging probes for noninvasive primary diagnosis, assisting histological grading, defining the extent and detecting recurrence of cerebral gliomas. FET-PET has shown promising results in differentiating tumor recurrence from therapy-associated contrast enhancement on MRI scans.

Aims: The aim of this retrospective review was to assess the ability of FET-PET in the confirmation of tumor recurrence in patients with contrast enhancement on MRI following initial multimodality treatment for high grade gliomas.

Methods: A retrospective review conducted on patients referred for FET-PET with suspected tumor recurrence on MRI in a single center during 2013 and 2014. All patients had high grade glioma (World Health Organization, WHO grade III/IV) and initially treated with neurosurgical resection, radiotherapy and/or chemotherapy. Image acquisition was performed 30–60 minutes after administration of 5 mCi (185 MBq) of FET. Tracer uptake was evaluated semiquantitatively with maximum tumor to mean brain ratio (TBR_{max}). TBR_{max} beyond the cut-off of 2.5 has been reported to have a high positive predictive value (98%) for detection of a neoplastic lesion and was considered positive in our center. The imaging results were correlated with histopathological findings, MRI and clinical follow-up.

Results: Seven patients were referred for FET-PET, and all had TBR_{max} value more than 2.5 (mean: 3.5 ± 0.8,range: 2.6–4.5) corresponding to gadolinium enhancement on MRI in the area of the primary tumor after initial treatment. Six patients (86%) had glioma recurrence either by histopathological confirmation (3 patients) or MRI and clinical progression (3 patients). One patient developed advanced radiation induced dementia and further radiological follow-up was withdrawn.

Conclusion: In our single center experience, FET-PET had significant impact on the management of patients with contrast enhancement on MRI after initial treatment of high grade gliomas, by assisting in differentiating recurrent tumor from radiation necrosis.

PO8
NERVOUS SYSTEM INVOLVEMENT BY RECURRENCE OF NON-HODGKIN LYMPHOMA ON FDG-PET/CT: LEPTOMENINGEAL DISEASE AND NEUROLYMPHOMATOSIS

A Iravani[1], C Bui[1], L Shen[1], R Mansberg[1,2]

[1]Department of Nuclear Medicine and PET, Nepean Hospital, Kingswood, Australia
[2]University of Sydney, Sydney, Australia

© 2015 The Authors
Internal Medicine Journal © 2015 Royal Australasian College of Physicians

Background: Systemic non-Hodgkin lymphoma (NHL) may involve the nervous system (NS) at every level, including central nervous system (CNS), such as leptomeningeal and parenchymal disease, and peripheral nervous system (PNS) such as cranial nerves, spinal nerve roots and peripheral nerves, also known as neurolymphomatosis. Whereas involvement of CNS complicates the course of a significant minority of patients, PNS involvement is rare and most episodes of NS involvement occur in the setting of relapsed NHL. Successful therapy is contingent on the recognition of these neurologic complications, yet the diagnosis is difficult and often elusive. Although only a limited number of case reports are available, the diagnostic yield of MRI and FDG-PET has been reported to be high, with abnormal findings found in 77% and 84%, respectively.

Aims: To illustrate the various patterns of NS involvement by relapsed NHL on FDG-PET in three patients and the role of FDG-PET in the diagnosis and selection of subsequent treatment strategy.

Methods and Results: In the first patient, FDG-PET discovered unsuspected CNS (cerebellar leptomeningeal) involvement, in addition to systemic disease. In the second patient, FDG-PET accurately demonstrated NHL recurrence confined to the cauda equina and thereby helped with selection of the appropriate treatment including targeted radiotherapy and intrathecal chemotherapy. In the third patient, FDG-PET demonstrated a rare case of NHL recurrence confined to the brachial plexus, despite interval response to the first line of therapy in other sites of disease. Salvage chemotherapy and stem cell transplantation were considered.

Conclusion: FDG-PET facilitates early recognition of these rare neurologic manifestations (leptomeningeal disease and neurolymphomatosis), defines the best target for biopsy (together with MRI findings) and provides further information regarding the extent of systemic disease, which in turn, help with selection of appropriate subsequent treatment and may improve outcome.

PO9
PIB IMAGING IN POSTERIOR CORTICAL ATROPHY: IS AMYLOIDOSIS CONTRIBUTING TO THE NEUROPATHOLOGY

M McCarthy[1], A Campbell[2], P Panegyres[3,4]

[1]Royal Perth Hospital, Department of Nuclear Medicine, Sir Charles Gairdner Hospital Department of Nuclear Medicine, Perth, Australia
[2]Royal Perth Hospital, Department of Biomedical Engineering and Physics, Perth, Australia
[3]Neurodegenerative Disorders Research Pty Ltd, Perth, Australia
[4]University of Western Australia, Perth, Australia

Background: Posterior Cortical Atrophy (PCA) is a progressive neurodegenerative disorder that initially presents as difficulties in higher visual processing with sparing of memory and insight. There can be significant variability in symptoms experienced and no standardised diagnostic criteria are used clinically. Controversy remains as to whether PCA is a unique disease or represents a variant of Alzheimer's disease (AD) with an atypical visual presentation. Pittsburgh compound B (PiB) imaging has confirmed amyloidosis in the majority of patients presenting with clinical features of PCA. No studies have shown an occipital predominance of amyloid, which might be expected in patients with visual and visual associative symptoms.

Aim: We present the imaging (MRI, FDG-PET, PiB and SUVR cortical maps) of 3 cases with a clinical presentation of PCA, who illustrate the discordance between symptoms and localised occipital lobe neuronal dysfunction and generalised cerebral amyloidosis.

Discussion: Neuronal dysfunction in Alzheimer's disease is thought related to the neurotoxic effects of cerebral amyloidosis. Generalised cerebral amyloidosis is often seen in seen in AD, Lewy Body Dementia (LBD), cerebral amyloid angiopathy (CAA), primary progressive aphasia (PPA) and also PCA, yet these conditions present with markedly different clinical features. Diffuse neuronal toxicity due to diffuse cerebral amyloidosis cannot explain the localise symptoms and marked metabolic dysfunction localised to the parieto-occipital cortex on FDG PET in PCA. This suggests a different underlying pathophysiology. Some authors have suggested a degenerative tractopathy as a cause for the localised visual and visual associative symptoms.

Conclusion: The presented cases highlight the discordance between the clinical and metabolic findings, which localise to the occipital visio-spatial cortex in PCA, and the diffuse distribution of cerebral amyloidosis. This again raises the question as to the role of amyloid as a bystander or as a significant contributant to the neurodegeneration.

P10
THE USE OF 18F-FDG PET/CT IN STATUS EPILEPTICUS – A CASE STUDY

S Saleem[1], J Welch[1], K Pathmaraj[1], S Lee[1], C Rowe[1]

[1]Austin Health, Melbourne, Australia

Background: Status Epilepticus (SE) is a life-threatening neurologic disorder that is essentially an acute, prolonged epileptic crisis. FDG PET/CT imaging of epilepsy has been restricted to the inter-ictal state, primarily because of the short half-life of FDG. However, in patients with very frequent seizures, ictal PET imaging may be possible. A 52-year-old female with past history of cerebral abscess treated surgically at the age of 13, with left frontal encephalomalacia and surrounding gliosis, presented with status epilepticus featuring right upper and lower limb myoclonus. The patient was unresponsive to pharmacological treatment and the FDG PET/CT scan was requested to localise the epileptic focus that may be amenable to surgical intervention.

Aim: To utilise FDG PET/CT imaging in determining the epileptic focus of a patient in SE.

Methods: The patient was intravenously administered with 235 MBq 18F-FDG and allowed to uptake in a dark room. 65 minutes post-injection, PET/CT imaging of the brain was performed on a Philips Gemini TF64. A low dose CT at 30 mAs, 120 kVp was performed for attenuation correction, followed by a 15 minute emission scan. The PET images were co-registered with MRI images for accurate anatomic localisation of hypermetabolic regions, to direct the neurosurgical team.

Results: The ictal PET study demonstrated intense hypermetabolic activity in the left precentral motor cortex. This area of hypermetabolism correlates well with the involuntary twitching of the patient's right hand and upper arm muscles. Localisation of the seizure focus led to resection of the left pre-and post-central gyrus. Post-surgery, the patient's condition has markedly improved, except for sporadic focal jerking in the fingers of the right hand.

Conclusion: This case study highlights the feasibility and added usefulness of ictal FDG PET/CT imaging in the management of SE, even though it may be logistically challenging to perform regularly.

P11
SEEING HALF THE PICTURE AND DIFFICULTIES IN RECALL: INVESTIGATION OF HOMONYMOUS HEMIANOPIA AND MINIMAL COGNITIVE IMPAIRMENT WITH STRESS AND REST CEREBRAL PERFUSION SPECT IMAGING

P Duong[1], M Dobson[1], J P Halpern[2], H Dixson[1], K Lee[1]

[1]Bankstown Lidcombe Hospital, Sydney, Australia
[2]The Lindfield Centre, Sydney, Australia

Background: A 67-year-old man presented with minimal cognitive impairment, possibly secondary to mood disorder, and right homonymous hemianopia for investigation. Symptoms included short term memory impairment, delayed decision making, verbal repetition and extreme light sensitivity in the absence of migraine. Vascular risk factors included hypertension and family history. MRI and MR angiography were normal.

Aim: To investigate the cause of cognitive impairment and right homonymous hemianopia using cerebral perfusion SPECT imaging.

Method: Rest and stress SPECT studies were acquired on separate days. For the stress study, the patient was given 1 g acetazolamide intravenously 20 minutes prior to tracer injection (1 GBq Tc-99 m Ceretec). SPECT studies were acquired on the GE670 with fanbeam collimators, and reconstructed iteratively with resolution recovery and attenuation correction. Statistical analysis was performed using Neurostat.

Results: Rest study demonstrated a large perfusion defect involving the left temporo-occipital cortex and white matter. There were smaller perfusion defects including the right associative occipital cortex, the parietal cortices bilaterally and the inferior frontal cortices bilaterally. The stress study demonstrated that the large left temporo-occipital cortex and white matter perfusion defect was more severe, consistent with vascular disease, reduced cerebral perfusion reserve, and explained the right homonymous hemianopia. The smaller mild right associative cortex defect was also larger on the stress

© 2015 The Authors
Internal Medicine Journal © 2015 Royal Australasian College of Physicians

study, consistent with an additional smaller area of reduced perfusion reserve. Bilateral parietal cortical perfusion defects were less evident on the stress study, which may indicate concomitant minimal cognitive impairment of the Alzheimer's type. Reduced perfusion in the inferior frontal cortices persisted which can reflect depressive states.

Conclusion: Cerebral perfusion SPECT imaging can be an especially useful tool in the investigation of minimal cognitive impairment and unexplained homonymous hemianopia. Stress imaging is particularly useful in demonstrating reduced cerebral perfusion reserve even when MRI and MR angiography are normal.

P12
CEREBRAL PERFUSION SPECT IMAGING IN THE INVESTIGATION OF VISUAL OBSCURATION AND MINIMAL COGNITIVE IMPAIRMENT: A CASE STUDY

S Musgrave[1], J P Halpern[2], H Dixson[1], K Lee[1]

[1]Bankstown Lidcombe Hospital, Sydney, Australia
[2]The Lindfield Centre, Sydney, Australia

Background: A 76-year-old man presented with visual obscuration and minimal cognitive impairment following a mitral valve replacement one year earlier. There were no ophthalmic causes for the wave distortion of vision, which occurred in both eyes and lasted seconds. They were not related to posture or activity. MRI showed gliosis and atrophy in the left temporoparietal region inferolaterally. Vascular risk factors include diabetes, hypercholesterolaemia, ischaemic heart disease and smoking.

Aim: To investigate the patient's visual obscuration and cognitive impairment.

Method: Rest and stress cerebral perfusion imaging were performed on separate days. For the stress study, the patient received 1 g acetazolamide (Diamox) intravenously, followed by 1 GBq of ^{99m}Tc HMPAO (Ceretec) 20 minutes later. Both rest and stress scans were acquired on a GE670 gamma camera using fanbeam collimators, iterative reconstruction and Chang's attenuation correction. Neurostat was used to perform statistical analysis.

Results: The resting study demonstrated a severe focal perfusion defect in the left posterior temporal cortex and white matter extending into the left occipital white matter. This was not evident on MRI and could explain the visual obscuration. There were mild perfusion defects in the parietal cortices bilaterally. The perfusion defects noted in the parietal cortices bilaterally on the rest study were larger on the stress study, consistent with reduced cerebral perfusion reserve and vascular disease, rather than Alzheimer's disease. The perfusion defect in the left posterior temporal cortex and white matter extending into the left occipital white matter persisted unchanged on the stress study.

Conclusion: The rest/stress cerebral perfusion imaging was valuable in this patient to investigate his visual obscuration and cognitive impairment, as it demonstrates reduced cerebral perfusion reserve. Vascular disease was considered more likely than Alzheimer's disease, and therefore the patient was vigorously treated for his multiple vascular risk factors.

P13
Corticobasal degeneration, a rare neurodegenerative disorder diagnosed early with the help of cerebral perfusion SPECT imaging

K Denmeade[1], DK Chan[2], K Lee[1]

[1]Bankstown – Lidcombe Hospital, Sydney, Australia
[2]The University of New South Wales, Sydney, Australia

Clinical History: A 75-year-old man presented post-fall with asymmetrical right upper limb apraxia with dystonia and right hand muscle wasting, decreased mobility and rigidity on the background of depression and mild cognitive impairment. The patient was being treated with anti-Parkinson's medications with no response. MRI and CT demonstrated no evidence of corticobasal degeneration (CBD).

Background: CBD is a rare neurodegenerative disease involving the cerebral cortices and extrapyramidal structures. Patients can present with Parkinsonian features, however, CBD is unresponsive to Parkinson's medications such as levodopa. Patients with CBD may also present with gradual apraxia of one limb, mild cognitive impairment and depression.

Aim: To investigate the possibility of CBD with cerebral perfusion SPECT in a patient unresponsive to anti-Parkinson's medications, despite no evidence of CBD reported on CT or MRI.

Method: Cerebral perfusion SPECT images were acquired one hour post-administration of 1 GBq Tc99m HMPAO over 24 minutes on the GE 670 camera with fan beam collimators. Images were iteratively reconstructed with Chang's attenuation correction and statistical analysis was performed using Neurostat.

Results: SPECT imaging demonstrated mild perfusion defects in the left caudate, right thalamus, left anterior parietal cortex, right prefrontal cortex, right internal frontal cortex and the right anteromesial temporal cortex. The most defining pattern of CBD demonstrated in this patient was the asymmetrical hypoperfusion of the contralateral basal ganglia (left caudate) to the asymmetrically affected limb (right arm). Additionally, characteristic patterns of HMPAO uptake in patients with CBD can include impaired perfusion in the putamen, thalamus, and all regions of the parietal cortex and frontal cortex, as was demonstrated in this gentleman. Frontal and temporal cortical perfusion defects may also be related to the patient's depression.

Conclusion: Cerebral perfusion SPECT may be a valuable tool in the early diagnosis of corticobasal degeneration including patients who may present with Parkinsonian features, apraxia of one limb, depression and mild cognitive impairment.

P14
FROM NEUROLITE® TO CERETEC® – A MAJOR HEADACHE

N-L Scott[1]

[1]Royal Brisbane and Women's Hospital, Brisbane, Australia

Background: ^{99m}Tc Neurolite (ECD), a brain perfusion agent, was withdrawn from the market in 2012 enforcing change to the only available alternative agent; ^{99m}Tc Ceretec (HMPAO). This simple change in imaging agent incited a massive overhaul in processes and procedures for brain perfusion studies, from the ordering of stock, right through to the interpretation of the images.

Aims: To highlight the differences in procedures and processes involved with changing to an alternative brain perfusion radiopharmaceutical. This includes the process of ordering stock, obtaining TGA approval, methods of manufacture and QC, shelf lives, kit activity, uptake times and image interpretation.

Method: Compare and contrast each step of the process involved with organising, manufacturing, acquiring and interpreting brain perfusion images for each imaging agent.

Results: Preliminary results indicate that changing to Ceretec meant the price of patient doses has increased. Extra paperwork (Special Access Scheme) is required for TGA approval of each patient dose. Extra steps are required in the reconstitution and quality control of Ceretec kits. There is a reduction of the shelf life of reconstituted Ceretec kits, and there is also the possibility of additional radiation exposure to patients as the imaging agents are not comparable.

Conclusion: The change from Neurolite to Ceretec was not simple. The availability of Neurolite in the future would be welcomed. Alternatively, the production of a new brain perfusion imaging agent would certainly be considered for use.

P15
68GA-DOTATATE PET/CT IN CONJUNCTION WITH 99MTC-HEAT DAMAGED RBC IMAGING – BRINGING BACK THE OLD WITH THE NEW

J Bell[1], T Watson[1], L Kete[1], T Anderson[1]

[1]Hunter New England Imaging, Newcastle, Australia

Background: Positron Emission Tomography/Computed Tomography (PET/CT) utilizing 68Gallium-DOTATATE is a well-established method to identify Neuroendocrine Tumours (NETs). 68Ga-DOTATATE is a somatostatin analogue that demonstrates a high affinity for somatostatin receptors commonly expressed on NETs. One drawback with this imaging technique is the inability to differentiate between NETs and normal cells which express somatastatin receptors, such as splenic tissue, the kidneys, the pituitary, and adrenal glands. We describe two cases where the combined use of 68Ga-DOTATATE PET/CT and 99mTc Heat Damaged Red Blood Cell (HDRBC) imaging was investigated to differentiate disease from normal variants.

Aim: To differentiate between NETs and splenunculi to ensure appropriate diagnosis and to optimise patient management and outcomes.

© 2015 The Authors
Internal Medicine Journal © 2015 Royal Australasian College of Physicians

Methods: Two patients with clinical suspicion of NETs underwent consecutive 68Ga-DOTATATE PET/CT and 99mTc Heat Damaged Red Blood Cell (HDRBC) scans.

Results: 68Ga-DOTATATE avid foci were identified in the pancreatic tail of both cases. Both patients underwent further imaging utilising 99mTc-HDRBCs to differentiate NETs from possible splenunculi. Patient 1 demonstrated 99mTc-HDRBC uptake at the location of the 68Ga-DOTATATE avid pancreatic mass. Patient 2 demonstrated normal biodistribution of 99mTc-HDRBCs and no uptake in the 68Ga-DOTATATE avid mass. 68Ga-DOTATATE scanning alone may have resulted in unnecessary surgery for this patient.

Conclusion: The utilization of 99mTc-HDRBC imaging in conjunction with 68Ga-DOTATATE PET/CT as complimentary imaging techniques conclusively defined the nature of the lesions directing appropriate management. In patients with positive 68Ga-DOTATATE findings it is imperative that splenunculus be excluded as a differential diagnosis.

P16
OPTIMISING THE DETECTION OF COLORECTAL CANCER LIVER METASTASES WITH DYNAMIC FDG PET ACQUISITIONS

P Thomas[1,2], N Dowson[3], C Baker[2,3], J Smith[1,3], S Rose[2,3]

[1]Nuclear Medicine Department, Royal Brisbane and Women's Hospital, Herston, Australia
[2]School of Medicine, The University of Queensland, St Lucia, Australia
[3]Australian e-Health Research Centre, Royal Brisbane and Women's Hospital, Herston, Australia

Background: FDG PET is commonly used prior to hepatic metastatectomy to ensure all the liver metastases are resectable and there are no other distant metastases that would render such curative surgery futile. The sensitivity for FDG PET for detecting liver metastases is suboptimal due to background liver activity and other confounding factors. As a result, many patients subsequently have recurrences post-hepatic resection.

Aims: To improve the detection of liver metastases with FDG PET by exploiting the different FDG handling characteristics of normal liver and metastases.

Methods: A sixty minute list mode PET acquisition over the liver was obtained in 8 patients immediately post-FDG injection, followed immediately by a conventional PET acquisition. The following data sets were generated and blindly read by an experienced nuclear medicine physician with a minimum 1 week separation between reads: Standard PET study, 30–60 minute post-injection summed static image, Ki image (standard 2 compartment kinetic model), Ki image (novel 'tubes' compartment model), and a slope image (subtraction of 30 from 60 minute image). Numbers of definite and probable metastases were counted in each lobe of the liver.

Results:

	Definite mets	Possible mets
30 minute static	19	1
Slope model	16	4
Kinetic model standard	17	3
Kinetic model tubes	18	2
Standard 2 min bed	17	5

The non-standard methods did not find metastases in lobes not involved on standard imaging.

Conclusion: The non-standard methods appear promising with subjective improvement in image quality and certainty appeared greater, however, a larger sample size would be required to demonstrate a significant difference in methodology.

P17
COMPARISON OF DOUBLE-INPUT COMPARTMENTAL MODELLING AND LOGAN PLOT METHODS FOR METABOLITE CORRECTION IN THE ANALYSIS OF DYNAMIC PET DATA: A SIMULATION STUDY

T.S. Koh[1,2], C.H. Thng[1,2], S.W.-K. Yu[3], L. Martarello[4], D.C.-E. Ng[3,2], Q.-S. Ng[5]

[1]Department of Oncologic Imaging, National Cancer Centre Singapore, Singapore
[2]Duke-NUS Graduate Medical School, Singapore
[3]Department of Nuclear Medicine, Singapore General Hospital, Singapore
[4]Roche Translational Medicine Hub, SingHealth Research Facilities, Singapore
[5]Department of Medical Oncology, National Cancer Centre Singapore, Singapore

Background: Dynamic PET scanning following intravenous injection of a suitable radiolabeled ligand (tracer) offers potential to quantify physiological parameters in vivo. Many radioligands can be metabolized in the body, with the metabolites carrying the radioactive label. The measured tracer time-activity curve (TAC) represents a mixture of authentic (parent) tracer and metabolites. In oncologic imaging where substantial radiometabolites can appear in both the arterial input and tumor TACs, appropriate correction for metabolite is warranted for quantitative assessment of the parent tracer. Double-input compartmental models (DICMs) have been proposed to concurrently account for the kinetics of both parent and metabolites in the tissue, which can involve about 6 or more parameters for curve-fitting. The double-input Logan method (LoganDI) offers a much simpler alternative for metabolite correction. It would be of interest to study whether parameter estimates derived from both methods are similar.

Aim: To investigate whether total volumes of distribution (parent V_T^p, and combined parent- metabolite V_T) obtained using DICM and LoganDI are correlated, by using computer simulation.

Methods: 5-[^{18}F]Fluorouracil (5-[^{18}F]FU) is a radiolabeled chemotherapy drug which metabolizes rapidly (~36% parent in 30 min). Synthetic data of 500 tissue TACs of 5-[^{18}F]FU were generated using a DICM (Fig. 1) by assuming a physiological range of human parameter values and parent-metabolite arterial input functions reported in the literature. Simulated tissue TACs were analyzed using the standard Logan plot and LoganDI to derive estimates of V_T and V_T^p, which were compared (by Pearson correlation) with those derived from DICM.

Results: V_T estimated from both standard Logan and LoganDI correlated well with DICM (r = 0.99), but only LoganDI exhibited possible quantitative correspondence (slope = 0.94). V_T^p estimated by LoganDI correlated well with DICM (r = 0.83, slope = 0.80).

Conclusion: LoganDI provides estimates of V_T^p and V_T for 5-[^{18}F]FU which correlate with those of DICM and may serve as a simpler alternative.

P18
DOES THE USE SUV_{MAX} UNCERTAINTY CHANGE BY REMOVING THE TIME OF FLIGHT (NON-TOF) RECONSTRUCTION ALGORITHM IN [^{68}GA]-PSMA PET IMAGING?

EA Bailey[1], E Hsaio[1], G Schembri[1], DL Bailey[1], P Roach[1]

[1]Royal North Shore Hospital, St Leonards, Australia

Aim: SUV_{max} in FDG PET whole body (WB) scanning is derived from a single pixel and is subject to statistical noise due to factors including choice of reconstruction algorithm, and attenuation and scatter corrections (AC &SC). The aim of this study is to measure the pixel standard deviation (SD) of SUV_{max} and to assess the impact of removing the ToF algorithm during reconstruction of the whole body [^{68}Ga]-PSMA PET scanning.

Method: Following injection of 100–150 MBq of [^{68}Ga]-PSMA, externally triggered gated (ETG) WB PET scans were acquired at 60 minutes and 2 to 2.5 hours on a ToF PET/CT (Siemens Biograph mCT64 × 64). Data were reconstructed into 6 gates initially using ToF 3D-OSEM with CT-based AC, SC and PSF recovery and then repeated removing only the ToF algorithm. Mean, SD and coefficient of variation (CoV) images were generated for both early and delayed imaging for both reconstructions. Regions-of-interest were placed over areas of assumed homogeneity (e.g., liver), blood pool, right normal parotid gland and bladder. For each ROI, SUV_{max} and SUV_{SD} (SD of the single pixel containing the SUV_{max}) values were determined.

Results: A total of 11 patients (delay n = 7) with mean injected dose 137 MBq (107–172 MBq) and weight 77.6 kg (64.7–106 kg) were included. As previously seen, the higher the uptake in tissue the lower the uncertainty in SUV_{max} with normal parotid and bladder showing the lowest noise estimates, increasing on delayed imaging. The Non-ToF data indicated a slight reduction in SUV_{max} uncertainty but not statistically significant. The CoV liver early imaging ToF versus non-ToF was 8% and 7.5% respectively, and delay imaging ToF versus non-ToF 11.8% and 11.9% respectively, higher than determined for FDG 4.2%[(1,2)].

© 2015 The Authors
Internal Medicine Journal © 2015 Royal Australasian College of Physicians

Table 1 Average SUV_{max} and CoV(SUV_{max} values of the 4 tissue sampled with and without ToF in the reconstruction algorithm (early n = 11; delay n = 7)

	Mean Value in Each ROI Location															
	Early Imaging								Delay Imaging							
	Normal Liver		Blood Pool		Bladder		Parotid		Normal Liver		Blood Pool		Bladder		Parotid	
	SUV_{max}	CoV	SUV_{max}	CoV	SUV_{max}	CoV	SUV_{max}	CoV	SUV_{max}	CoV	SUV_{max}	CoV	SUV_{max}	CoV	SUV_{max}	CoV
ToF	5.0	8%	1.5	20.2%	25.4	4.8%	15.6	3.6%	3.7	11.5%	1.0	38%	12.8	9.8%	13.3	5.3%
NToF	5.0	7.5%	1.4	19.1%	25.5	7.1%	15.4	4.5%	3.7	11.9%	1.0	45%	12.5	10.8%	13.6	7.9%

Conclusion: This methodology directly measures the uncertainty in reconstructed pixel values due to instrumentation and technical factors. Further uncertainties may be present related to other uncontrolled physiologic and tracer uptake properties. The use of time of flight in the reconstruction algorithm has very little impact on SUV_{max} uncertainty in this small cohort of patients and validates results previously shown with [^{68}Ga]-Dotatate. As expected, higher noise estimates were seen on delayed imaging, most likely due to the shorter half-life of Ga-68.

P19
MEASUREMENT OF TIME-OF-FLIGHT TIMING RESOLUTION FOR PHILIPS GEMINI TF64/INGENUITY TF128 PET/CT SYSTEM

G O'Keefe[1], P Jackson[1], K Hickson[1], S Gong[1]

[1]Molecular Imaging and Therapy, Austin Health, Melbourne, Australia

Background: As part of the daily Quality Control regime of Philips Gemini and Ingenuity TF PET/CT systems, a measurement of the Time-of-Flight timing resolution is reported.

Aims: As with all vendor supplied QC measures, independent verification of dailyQC results is required. Presented herein are the means of independently verifying the ToF timing resolution values reported by the Philips Gemini/Ingenuity TF class of PET/CT systems.

Methods: A collimated 22Na point source is displaced along the diameter of the PET system and the timing offsets observed in the timing data of the listmode events is used to calibrate the timing data. Following the calibration process, a measurement of the timing resolution in the centre of the Field-of-View of the PET system is made following the same method as used for the dailyQC measurement. As for the calibration stage of the measurement, the listmode events then have the timing data extracted on an event-by-event basis to generate a timing histogram for subsequent peak and width analysis. The Histogrammed ToF timing data are fitted using the Matlab™ Curve Fitting toolbox using a Gaussian function with a uniform background.

Results: A series of measurements was made on the Gemini TF64 and Ingenuity TF128 prior to and immediately after the annual service calibrations. The results of this analysis yielded values of 590 and 554 psec for the Gemini TF64 and Ingenuity TF128 respectively. By comparison, the Philips DailyQC reported 549 and 513 psec for the Gemini TF64 and Ingenuity TF128 respectively. In both cases, a discrepancy of approximately 8%.

Conclusions: A method is presented for measuring the Philips Gemini TF64 and Ingenuity TF128 TOF timing resolution independently. Based on these methods, there is a discrepancy of approximately 8% between the reported DailyQC and the results from the presented method.

P20
USE OF DIRECT INTRANODAL INJECTION OF ^{99M}TC-RHENIUM COLLOID FOR LYMPH NODE LOCALISATION: A CASE STUDY

B Chappell[1], J Toohey[1], A Poon[1], ST Lee[1], A Scott[1]

[1]Austin Health, Melbourne, Australia

Background: A 73 year old male with a history of pulmonary fibrosis and recently resected scalp and right ear squamous cell carcinoma (SCC) presented in December 2014 for a ^{18}F-FDG PET scan for disease restaging. The scan showed FDG-avid bilateral neck lymph nodes, and further FDG-avid lymph nodes in the thorax, abdomen and axilla likely due to either metastatic SCC spread or granulomatous disease related to his pulmonary fibrosis. Subsequent fine needle aspiration of the left neck and right axilla showed malignant SCC in neck nodes, however right axilla samples were not diagnostic. To determine whether FDG-avid lymph nodes distant to the neck were metastatic SCC, which would impact on management, a surgical biopsy of the right axilla was planned. To guide biopsy, an intra-nodal injection of ^{99m}Tc-Rhenium Sulphur Colloid of the FDG-avid axillary lymph node was performed.

Method: Prior to surgery and under ultrasound guidance 9MBq of ^{99m}Tc-Rhenium Colloid (1 ml volume) was injected into the most prominent right axilla lymph node correlating to the most FDG-avid lymph node. Following injection the patient underwent SPECT/CT imaging of the axillae and thorax; the patient's PET/CT scan position was duplicated to allow for direct image comparison.

Results: Comparison of SPECT/CT and PET/CT imaging confirmed successful intra-nodal injection of the FDG-avid right axilla lymph node. The lymph node was successfully localised intra-operatively using a gamma probe and was excised. Ex-vivo imaging using the Sentinella® mobile gamma camera further confirmed successful excision. Post-surgery node histology showed non-necrotising granulatous inflammation in keeping with lymphoproliferative pulmonary fibrosis with no evidence of malignancy. Confirmation of distant FDG-avid disease as being granulomatous and not metastatic spread allowed for planned Head/Neck radiation therapy to treat the patient's metastatic SCC.

Conclusion: The inclusion of direct presurgical intra-nodal 99mTc-Rhenium Colloid injection improved diagnostic certainty and directly impacted on patient management.

P21
PRE-OPERATIVE LYMPHOSCINTIGRAPHIC MAPPING FOR LYMPH NODE TRANSFER IN PATIENTS WITH POST-MASTECOMY LYMPHOEDEMA

A Culverson[1], K Sek[1]

[1]Sir Charles Gairdner Hospital, Nedlands, Australia

Background: Lymph node transfer is an emerging technique in improving lymphatic function of patients with post-mastectomy lymphoedema. Although the superficial inguinal nodes for transfer that drain the lower abdominal wall are harvested, a number of studies have reported changes to the lymphatic function in the donor limb after lymph node transfer in some patients.

Aims: The aim of the lymphoscintigraphy study was: 1. Provide pre-operative assessment of arm lymphoedema. 2. Map lymphatic drainage of lower extremities to guide lymph node harvest, minimising risk of lymphoedema in the donor limb.

Methods: Five patients had lymphoscintigraphic assessment the day prior to planned lymph node transfer surgery. 15 MBq Tc-99m Calcium Phytate Colloid was injected intradermally between the 2nd interdigital webspaces of both hands. Dynamic imaging was acquired for 30 mins. 60 MBq of Tc-99m Calcium Phytate Colloid was injected intradermally between the 1st interdigital webspaces of both feet and dynamic imaging following radiotracer drainage from feet to pelvis was acquired. Wholebody scans were acquired at approximately 1 hr and 3 hrs post-hand injection. Gamma probe was used in surgery to identify and avoid lymph nodes draining the lower extremity. SPECT-CT was also used when anatomical visualisation of lymph nodes was required.

Results: Two patients demonstrated bilateral lymphatic drainage in the upper extremities and as a result did not undergo lymph node transfer. One

© 2015 The Authors
Internal Medicine Journal © 2015 Royal Australasian College of Physicians

patient underwent microvascular lymph node transfer to the right wrist, while 2 patients underwent vascularised lymph node flap transfer to the right axilla. On 3 month follow up none of the patients who underwent lymph node transfer have developed clinical signs of lymphoedema in the donor limb.

Conclusion: Lymphoscintigraphic mapping and use of a gamma probe may assist surgeons in identifying and avoiding lymph nodes draining the lower extremity and reduce the risk of iatrogenic lympoedema.

P22
CONCURRENT LOW DOSE MYOCARDIAL PERFUSION IMAGING (MPI), CORONARY ARTERY CALCIUM SCORING (CACS) AND CT CORONARY ANGIOGRAPHY (CTCA) IN THE MANAGEMENT OF CORONARY ARTERY DISEASE (CAD): INITIAL EXPERIENCE WITH AN ULTRALOW DOSE SPECT-CT SCANNER

R Alipour[1], B Elison[1], E Hasche[2], R Dunn[2], P Burnett[2], H Dixson[1], C Bui[1], QL Chiam[1], J Behn[1], K Denmeade[1], Kien Lee[1]

[1]Department of Nuclear Medicine and Ultrasound, Bankstown-Lidcombe Hospital, Bankstown, Sydney, Australia
[2]Cardiology Department, Bankstown-Lidcombe Hospital, Bankstown, Sydney, Australia

Background: Anatomical and functional imaging are useful in the investigation of CAD. In CTCA, the number of proximal segments with mixed or calcified plaques and >50% stenoses are the best prognostic parameters. MPI and CACS provide independent and complementary prognostic indicators of short- and long-term cardiac events.

Aims: To correlate CTCA with MPI and CACS performed concurrently in two groups of patients, either with no known CAD or with known CAD and previous revascularisation.

Methods: The first 60 consecutive patients referred for concurrent low dose MPI, CACS and CTCA were studied. Patients were scanned using low dose ultrafast GE570c cadmium-zinc-telluride SPECT-CT (64-slice CT with adaptive statistical iterative reconstruction). CTCA and MPI images were co-registered (CardIQ Fusion). Six patients did not have CACS due to previous coronary revascularisation.

Results: Technically satisfactory studies were obtained in all patients.

In the group with no known CAD (N = 54), 2 of the 4 patients with >50% proximal stenoses had reversibility on MPI (mean CACS 542.75, SD ± 313.95); none of the 30 patients with <50% stenoses in the proximal segments had reversibility on MPI (mean CACS 301, SD ± 326.74); and 20 patients had normal CTCA, normal MPI and CACS of 0. In the group with known CAD and previous revascularisation (N = 6), one patient had patent grafts and reversibility in the non-grafted territory on MPI (native vessel >50% stenosis); one patient had >50% stenosis proximal to the stent as well as in-stent stenosis with reversibility in the corresponding territory on MPI; and 4 patients had patent grafts or stent(s) and no reversibility on MPI. Mean radiation dose for MPI including CACS was 3.4 mSv (SD ± 1.28 mSv), and for CTCA alone was 2.6 mSv (SD ± 1.36 mSv).

Conclusion: Concurrent anatomical and functional cardiac imaging was technically feasible in all patients, associated with low radiation doses and provided diagnostic and prognostic information.

P23
THE UTILITY OF MIBG SCINTIGRAPHY IN THE DIAGNOSTIC ALGORITHM FOR PATIENTS WITH SUSPECTED PHEOCHROMOCYTOMA – A TERTIARY HOSPITAL AUDIT

R Gauci[1,2], N Loh[1], E M Lim[2,3]

[1]Nuclear Medicine Department, Sir Charles Gairdner Hospital, Perth, Australia
[2]Endocrinology Department, Sir Charles Gairdner Hospital, Perth, Australia
[3]Biochemistry Department, Pathwest QEII, Perth, Australia

Background: Pheochromocytoma and paragangliomas arise from chromaffin cells in the adrenal medulla or sympathetic ganglia. Diagnostic work-up includes biochemical testing and imaging. Plasma metanephrines provide a highly sensitive test however false positives remain a problem. A recent meta-analysis indicates I-123 Meta-iodobenzylguanidine (MIBG) scintigraphy has sensitivity and specificity greater than 90% for detection of neuroblastoma and pheochromocytoma. Recent literature has attempted to elucidate the role of MIBG scintigraphy in the work up of pheochromocytoma. Newly published guidelines recommend its use in patients who are planned to have I-131 treatment. Other indications include patients at increased risk of metastatic disease, extra-adrenal disease, multifocal or recurrent disease. 18-FDG PET is preferred over I-123 MIBG in patients with known metastatic paraganglioma. The management of a patient with a mildly positive result is debateable; options include clonidine suppression testing, wait-and-retest approach, or proceeding directly to imaging studies. The nature of this decision is often based on pretest probability, clinical history and judgement.

Aims: To examine utility of MIBG scintigraphy in the diagnostic algorithm for the investigation of patients with suspected pheochromocytoma.

Methods: A retrospective case series of all patients who underwent MIBG scintigraphy at a tertiary hospital for suspected phaeochromocytoma since January 1, 2009. Clinical, biochemical and imaging data was gathered from medical records and PathWest pathology database. Subgroup analysis of discordant biochemical and imaging results were compared to a histopathologic gold-standard.

Results and Conclusion: 59 scans from 53 patients were included in the analysis. The age of the patients at the time of study ranged from 17 to 88 years of age, the mean and median were both 57 years. 35 of 59 (59%) scans demonstrated MIBG-avid pheochromocytoma or paraganglioma. The most commonly prescribed medication was phenoxybenzamine. Further results are pending statistical analysis and will be presented in full at the meeting.

P24
HIGH DOSE MIBG THERAPY UNDER GENERAL ANAESTHESIA IN A 2 YR OLD CHILD

C Green[1], J Trpezanovski[1], G McCowage[2], R Howman-Giles[1,3]

[1]Department of Nuclear Medicine, The Children's Hospital at Westmead, Westmead, Australia
[2]Department of Oncology, The Children's Hospital at Westmead, Westmead, Australia
[3]Sydney Medical School, University of Sydney, Sydney, Australia

Background: High dose ^{131}I-MIBG therapy is increasing being applied in neuroblastoma patients who are refractory to initial induction therapy or who have recurrence of disease after therapy. Practical issues with small children and infants make this form of therapy difficult particularly due to compliance in the isolation room and radiation safety issues for parents, carers and staff.

Aims: Description and discussion of issues relating to high dose MIBG therapy in a child who required general anaesthesia for the therapy.

Methods: A 2 yr old male presented with abdominal distention and was diagnosed with Stage IV neuroblastoma. He had a large abdominal tumour and extensive metastatic disease in bone/bone marrow/soft tissue sites which were avid on ^{123}I-MIBG scans. He had 7 cycles of induction chemotherapy but had a moderate partial response. His treatment plan was to surgically de-bulk the primary tumour, followed by high dose ^{131}I-MIBG therapy, high dose chemotherapy, autologous bone marrow transplant, radiotherapy and immunotherapy.

Results: Due to his personality and separation anxiety it was decided that sedation would be unpredictable and he should be anaesthesised. Extensive consultation occurred between ICU, anaesthestics, nuclear medicine, oncology and parents. As general anaesthesia was not performed outside of specialised units within the hospital, a formal protocol was created including education of personnel in each unit, oncology staff and parents regarding radiation safety. After 2 weeks recovery from extensive surgery, he received 666 MBq/kg of ^{131}I-MIBG (7655 MBq). He tolerated the therapy well and had a post-therapy scan under sedation on day of discharge.

Conclusion: High dose MIBG therapy is a complicated procedure particularly in infants and young children. Our patient has progressed through the therapy without complications and has had a significant response to the planned treatment program. His most recent MIBG scans show continuing resolution of metastatic disease.

© 2015 The Authors
Internal Medicine Journal © 2015 Royal Australasian College of Physicians

P25
^{99M}TC-LABELLED D-GLUCOSAMINE IN THE EVALUATION OF DISEASE ACTIVITY IN PATIENTS WITH ANKYLOSING SPONDYLITIS AND RHEUMATOID ARTHRITIS

A Markewycz[1], S Angelides[1], N Manolios[2], M Ali[2], B Camden[1], E Eflaki[2], K Pavic[2], R DeCosta[3]

[1]Nuclear Medicine, Westmead Hospital, Sydney, Australia
[2]Departments of Rheumatology, Westmead Hospital, Sydney, Australia
[3]Radiology, Westmead Hospital, Sydney, Australia

Background: The assessment of disease activity in inflammatory arthritic conditions such as rheumatoid arthritis (RA) and ankylosing spondylitis (AS) using imaging is essential in order to detect early disease and monitor therapy.

Aims: The aim of this study was to evaluate the clinical utility of a novel radiotracer, ^{99m}Tc-Glucosamine, and its role in the assessment of disease activity for both RA and AS.

Methods: 25 RA patients and 12 patients with AS of various stages of disease were recruited into the study. Whole body and static images were acquired at 15 min and 3 hrs using a dual-head Siemens Symbia SPECT/CT gamma camera following an intravenous 600 MBq injection of ^{99m}Tc-Glucosamine. Images were analysed by a nuclear physician and each joint given a score (0–5) based on the tracer uptake. Glucosamine scans were then compared to other routinely used imaging tests such as MRI, bone scans and correlated with clinical activity.

Results: In AS patients, active sacroiliitis was observed in three patients on the ^{99m}Tc-Glucosamine scans. However, scan findings correlated variably with clinical parameters and other imaging modalities. ^{99m}Tc-Glucosamine scans were more adept at identifying active disease and differentiating inflammatory manifestations of disease from non-inflammatory causes. In RA, ^{99m}Tc-Glucosamine accumulated at all known sites of disease involvement. Uptake was most pronounced in the patients with active untreated disease. Relative tracer activity at involved joints increased over time. Using Spearman's correlation co-efficient there was a positive correlation between glucosamine scan scores, CRP ($p = 0.048$) and clinical assessment ($p = 0.003$) that was not noted with bone scans.

Conclusion: The radiotracer was well tolerated by all patients with no adverse events. ^{99m}Tc-Glucosamine imaging can detect spinal inflammation in AS. With respect to RA, ^{99m}Tc-Glucosamine is a viable option to bone scans for imaging inflamed joints showing a significant correlation between clinical evaluation of patients with RA and scan results.

P26
DMSA SCAN IN ATHEROEMBOLIC RENAL DISEASE

A Woodcock[1], Q Chiam[1], H Dixson[1], R Alipour[1], T Spicer[2], K Lee[1]

[1]Department of Nuclear Medicine & Ultrasound, Bankstown-Lidcombe Hospital, Sydney, Australia
[2]Department of Renal Medicine, Bankstown-Lidcombe Hospital, Sydney, Australia

Background: Cholesterol crystal embolism (CCE) or atheroembolism occurs when cholesterol from an atherosclerotic plaque is dislodged (often during angiography), and obstructs blood vessels. This can cause skin conditions such as livedo racemosa, gangrene of the extremities and sometimes renal failure. CCE can be diagnosed by renal biopsy. When the kidneys are involved, the disease is referred to as atheroembolic renal disease (AERD).

Case Report: A 72 year old male presented with asymptomatic acute renal failure two weeks after coronary angioplasty. On presentation he was lethargic, hypertensive (190/110 mmHg) and had an elevated creatinine of 214 μmol/L with an estimated Glomerular Filtration Rate (eGFR) of 26 ml/min ($N \geq 90$ ml/min/1.73 m^2). His renal function rapidly deteriorated with creatinine rising to 625 μmol/L and eGFR dropping to 6 ml/min. His renal ultrasound, WCC and CRP were normal and urine microscopy was negative for casts or dysmorphic cells. The differential diagnosis was contrast nephropathy, ACE inhibitor nephrotoxicity or cholesterol embolism, with the latter suspected due to a rise in eosinophils and new livedo racemosa (mottled skin appearance) of feet and toes. A renal biopsy could not be performed due to the recent coronary artery drug eluting stent insertion requiring antiplatelet therapy, so a DMSA scan was requested. The DMSA scan showed reduced uptake in both kidneys with increased background activity, consistent with moderate to severe renal impairment. Focal photopaenic cortical defects were seen in both kidneys on SPECT/CT, most likely due to cholesterol emboli. Skin biopsies of the feet demonstrated multiple cholesterol emboli occluding arteries and arterioles within the submucosa and dermis.

Conclusion: The DMSA SPECT/CT study demonstrated multiple, focal photopaenic renal cortical defects consistent with cholesterol emboli. This supported the final diagnosis of AERD as the cause of the patient's renal failure.

P27
CAN ACQUISITION TIME BE SHORTENED IN HEPATOBILIARY SCINTIGRAPHY FOLLOWING ADMINISTRATION OF ENSURE PLUS® TO ASSESS GALLBLADDER EJECTION FRACTION?

K Devitt[1], EA Bailey[1], P Roach[1]

[1]Royal North Shore Hospital, St Leonards, Australia

Background: Hepatobiliary scintigraphy is used to assess the patency of the cystic duct and biliary system and is indicated in patents with suspected acute cholecystitis or common bile duct obstruction. Following withdrawal of Cholecystokinin (CCK) as the preferred agent to contract the gallbladder (GB), Ensure Plus® has been used based on the Ziessman[1] protocol. The aim of this study is to review the acquisition time needed to accurately assess gallbladder EF and if the current 60 minute acquisition could be reduced.

Method: A retrospective review of studies performed over a 2 year period following the introduction of Ensure Plus® to replace CCK was undertaken. Following administration of 200 MBq [^{99m}Tc]-Disofenin (DISIDA), a 60 minute dynamic acquisition was done to visualize filing of the gallbladder and bowel activity. Once GB was seen the patient drank 237 mL Ensure Plus® as the fatty meal replacement with a further 60 minute dynamic study acquired. Using the Siemens esoft MI Application package, gallbladder ejection fractions were calculated at 20, 30, 40 and 60 minutes with the mean EF determined at each timepoint. The studies were then divided into normal (≥40%), abnormal <33%) and equivocal (33 to 40%) using the 60 minute GB EF.

Result: A total of 33 studies were analysed with 4 excluded due to early termination of the acquisition. The mean gallbladder EF (n = 29) at 20, 30, 40 and 60 minutes was calculated as 28%, 38%, 46% and 53% respectively. When the data were divided based on normal, equivocal and abnormal gallbladder EF at 60 minutes (as seen in Table 1), the same result could be determined at 40 minutes for both the normal and abnormal group, with the GB EF curve appearing to plateau between 30 and 40 minutes for both groups.

Table 1 Summary of mean Gallbladder EF (%) calculated at 20, 30, 40 and 60 minutes following administration of Ensure Plus

	Mean Gallbladder EF (%)			
	20 min	30 min	40 min	60 min
Normal (n = 20)	35	47	56	64
Equivocal (n = 3)	12	23	27	35
Abnormal (n = 6)	12	18	21	26

Conclusion: Based on these results, the study acquisition could be shortened to 40 minutes in the majority of cases. However, as expected those patients with an equivocal study may require the full 60 minute acquisition. The mean gallbladder EF at 60 minutes for this cohort of patients was 53%, lower than that reported by Ziessman (62.6%) which was determined using normal subjects.

P28
SCINTIGRAPHIC METHODS TO RULE OUT HEPATIC NEOPLASMS

L Baker[1], B Goodwin[1]

[1]Nuclear Medicine & PET Department, The Townsville Hospital, Townsville, Australia

Background: Fibrolamellar hepatocellular Carcinoma (FHCC) is a rare form of hepatocellular carcinoma (HCC) that typically affects young adults and is characterised, under the microscope, by laminated fibrous layers interspersed between the tumour cells and differ from conventional HCC as

© 2015 The Authors
Internal Medicine Journal © 2015 Royal Australasian College of Physicians

they are non-encapsulated, but well circumscribed. A Liver Colloid & Hepatobillary scan was requested on a 27 yr old female suffering from epigastric pain with a recent history anorexia, nausea, malaise and myalgia.

Aim: Previous magnetic resonance and ultrasound imaging showed an incidental lesion in segment 5/6 of the liver. An international liver expert (family friend of the patient) requested nuclear medicine scans for assessment/characterisation of the lesion.

Methods: Planar and SPECT/CT images were performed following the injection of 213 MBq Tc 99m Calcium Phytate Colloid SPECT images were fused to the MRI performed 5 days prior. A Hepatobillary scan was performed 48 hr later to aid in the diagnosis. Dynamic and delayed images were performed following the injection of 244 MBq Tc 99m DISIDA and 250 ml full cream milk after 60 mins of initial imaging.

Results: Colloid scan – radiotracer uptake within the large exophitic lesion in the inferior pole of the liver is heterogeneous with more prominent uptake in the inferolateral aspect. Photopenia is present centrally in the area suggestive of scarring as seen on MRI. Radiotracer uptake within the right lobe liver is normal. Hepatobillary Scan –Large mass adjacent the lower pole of the right lobe of liver showing increased perfusion, increased uptake and delayed clearance. With normal tracer uptake within the remainder of the liver.

Conclusion: Based on the results of the two nuclear medicine procedures performed we were able to aid in characterizing the lesion within segments 5/6 of the liver and rule out FHCC, with the lesion more likely being focal nodular hyperplasia due its classic scintigraphic appearance.

P29
DEVELOPMENT OF SIMPLE COLONIC TRANSIT STUDY PROTOCOL AND ANALYSIS/DISPLAY WORKFLOW USING SIEMENS SOFTWARE AND EXCEL

J Maggs[1], B Goodwin[1], S Gibson[1]

[1]The Townsville Hospital, Townsville, Australia

Background: Disorders of Gastrointestinal (GI) transit and motility are common. Symptoms of delayed transit overlap with those of accelerated transit and more than one region of the GI tract may be affected. Measuring both the overall and regional colonic transit time is one of the most basic and primary tools in evaluating disorders of colonic motility.

Aims: To develop a simple way of imaging/processing/displaying the colonic transit of ingested Gallium 67 that gives an overall quantitative display of Gallium through the Whole Colon as well as the percentage (decay corrected) of ingested Gallium retained in 5 regions – precolon, ascending, transverse, descending and rectosigmoid colon.

Methods: The method used previously was a package on the ADAC Forte Scanner. With the installation of 2 Siemens scanners we investigated different methods of acquisition using medium and high energy general purpose collimators, with and without markers, with and without background subtraction, with and without motion correction. An excel spreadsheet with formulae and graphic display was developed to easily calculate and display the relative percentages, within the various regions, of initial Gallium ingested.

Conclusion: An excel spreadsheet and Siemens Savescreens sent to Impax provide an easily interpretable method of objectively assessing the transit of contents through the various regions of the colon.

P30
REVIEW OF EARLY AND DELAYED IMAGING PROTOCOL FOLLOWING LOW DOSE RADIOIODINE ABLATION – DOES IT CHANGE SENSITIVITY?

A Cluff[1], M Johnson[1], R Sambell[1], S Hain[1], A Lau[1], E Bailey[1]

[1]Royal North Shore Hospital, St Leonards, Australia

Background: Radioiodine ablation therapy is standardly used post-thyroidectomy to treat remnant thyroid cancer and metastatic deposits. Lower doses are increasingly being used, especially in low risk younger patients and small disease burden. Imaging is used to assess confirm uptake in residual tissue and to assess for possible metastatic spread. The aim of this study was to determine if the inclusion of early and delayed imaging changed lesion detectability and overall sensitivity.

Method: A retrospective review of patients treated with 1–2 GBq of radioiodine over a 12 month period with whole body and 5 min planar neck/chest imaging obtained at both 24 hrs and day 5–7 post-ablation were included. Data were randomized and reviewed by one experienced nuclear medicine physician and the nuclear medicine advanced trainee to identify the presence of I131 uptake in residual thyroid and other sites of disease. A 5 point scale (1 = not confident to 5 = very confident) was used to assess reporter confidence. Dose rate the patients were recorded at 24hr to assess exposure rates to staff during initial imaging.

Result: A total of 15 patients (M = 3, F =1 2) with Papilliary Thyroid Carcinoma (n = 10) or Follicular Thyroid Carcinoma (n = 5) were treated using 1–2 GBq radioiodine either with thyroid hormone withdrawal (n = 3) or an artificial stimulation (n = 12) protocol. On planar neck/chest imaging, a total of 14 lesions were identified on both 24 hour and delayed imaging. The number of lesions seen in the neck/chest on whole body imaging increased from 14 to 17 on delayed imaging with an additional 2 metastatic sites (anterior mediastinum and left midline chest) seen on delayed whole body imaging only in the five patients reviewed. Reporter confidence improved from 4 to 5 on delayed imaging, being not statistically significant. Patient dose rate was below 10 μSv/hr at the early and delayed timepoint, being 5.1 and 1.9 μSv/hr respectively.

Conclusion: The inclusion of 24 hour planar and whole body imaging does not improve lesion detectability and in some instances decreased reporter confidence. Therefore, the implementation of a delayed imaging only protocol will likely improve sensitivity for detecting sites of metastatic disease and reduce radiation exposure to the technologist.

P31
EMERGING ROLE OF BREMSTRAHLUNG SPECT/CT IMAGING IN YTTRIUM-90 RADIOSYNOVECTOMY

A Mazar-Atabaki[1], R Mansberg[1], R Russo[1]

[1]Nuclear Medicine Department, Concord Hospital, Sydney, Australia

Background: Yttrium-90 radiosynovectomy has been a therapeutic option in the management of monoarticular proliferative arthropathy for decades. Post-therapy imaging has been used to confirm successful administration of tracer to the affected joint and to image extravasation at the joint, draining lymph nodes and the liver, however the benefit has been limited by the poor imaging characteristics of Yttrium-90.

Aims: To evaluate the role of Bremstrahlung SPECT/CT imaging in Yttrium-90 Radiosynovectomy in confirming successful therapeutic administration and assessment of extravasation.

Methods: Patients referred for radiosynovectomy were assessed and treated in the conventional manner. Following intra-articular in administration of Yttrium-90 patients were arrested in the supine position for 72 hours. Regular planar images were performed of the treated joint, draining lymph nodes and the liver. In addition Bremstrahlung SPECT/CT of the treated joint was performed and the images were compared with the planar images.

Results: The result of the initial cohort of patients will be presented.

Conclusion: Bremstrahlung SPECT/CT imaging in Yttrium-90 Radiosynovectomy may benefit patients undergoing this therapy by more accurate imaging of treated joints. This may result in better and more specific localisation of extravasation which could benefit patients by instituting earlier and more specific therapy.

P32
SPECT/CT SUV – TECHNOLOGISTS EXPERIENCE USING A COMMERCIALLY AVAILABLE SOFTWARE PACKAGE

S Sam[1], E Stoakes[1], P Lin[1]

[1]Nuclear Medicine & PET Department Liverpool Hospital, Sydney, Australia

Background: The standardised uptake value (SUV) is a semi-quantitative tool that is routinely used in pet emission tomography (PET) to monitor treatment response. The use of SUV for single photon emission computed tomography (SPECT) however is not as common. To be able to generate meaningful SUVs the scanner needs to be properly calibrated, variables in patient demographics need to be accounted for and measurement of injected doses must be accurate. GE has available a software package (Q.Metrix) that applies the same principles from PET SUV calculation to SPECT data in turn enabling absolute values to be generated and used.

Aim: The aim of this study was to check the feasibility of using a SPECT quantitation package and discuss initial experiences from the Technologist's perspective.

© 2015 The Authors
Internal Medicine Journal © 2015 Royal Australasian College of Physicians

Methods: A database search was undertaken to find patients who had undergone both a PET/CT scan and a ^{123}I MIBG SPECT/CT scan. 6 patients met this criteria. PET lesion SUVs were taken from the approved reports. SPECT lesion SUVs were generated from the Q.Metrix program. The variables of camera sensitivity, patient demographics as well as injected/scan time were entered into the system. The program then automatically applied motion correction, and attenuation/scatter correction. SUVs results were tabulated.

Results: Of the 6 studies reviewed, 2 had concordant positive findings, 1 had discordant findings and 3 scans had concordant negative findings (Table 1).

Table 1

	PET SUV	SPECT SUV
Concordant Positive Scans	3.9	6.8
	13.2	7.7
Concordant Negative Scans	N/A	1.6
	N/A	0.9
	N/A	0.9
Discordant Scans	12.3	1.2

Conclusion: The Q.Metrix program easily generated SUVs from SPECT/CT data that correlated to concordant findings on PET/CT in 2 cases. This has the potential to allow for quantitative monitoring of therapy response in various SPECT/CT scenarios.

P33
THE VALUE OF SPECT/CT IN THE CHARACTERISATION OF SCAN FINDINGS – FROM DISEASE TO PHYSIOLOGICAL VARIANT

B.K.Vaughan[1], M.A. Rossleigh[1]

[1]Department of Nuclear Medicine and PET, Prince of Wales and Sydney Children's Hospital, Sydney, Australia

Background: A 52 year old man presented for a PET/CT study following the diagnosis of oesophageal carcinoma involving the distal third of the oesophagus. The primary malignancy was mildly FDG avid and there were two retrocrural lymph nodes that did not accumulate FDG. There was focal uptake in a calcified nodule at the posterior aspect of the right thyroid lobe, which warranted further investigation. The patient underwent an Ivor Lewis oesophagogastrectomy resulting in a gastric pull through. He was also treated with chemoradiotherapy. Follow-up of the thyroid nodule by ultrasound demonstrated a calcified right lobe nodule measing 15 × 14 × 20 mm in size. The final histology was follicular carcinoma of the thyroid with vascular invasion.

Method: In view of the vascular invasion, a 2.72 GBq dose of 131-Iodine was administered. A whole body I-131 scan and SPECT/CT study of the thorax was performed on a Phillips Brightview 5 days following the therapy.

Results: The whole body study demonstrated an unusual pattern of uptake in the right hemithorax medially, in addition to the expected uptake in the residual functioning thyroid tissue in the thyroid bed. The SPECT/CT identified that the unusual uptake in the thorax corresponded to physiological uptake within the stomach located in the thorax following the Ivor-Lewis oesophagogastrectomy.

Conclusion: The addition of SPECT/CT to standard planar imaging has significantly increased the specificity of scintigraphy. A scan appearance that may have been interpreted as metastatic disease was determined to be a physiological variant following surgery due to the information provided by the SPECT/CT study.

P34
CT DOSE IN SPECT/CT BONE SCANS

T. Beveridge[1], P. Marks[1], A. Wallace[1]

[1]Australian Radiation Protection and Nuclear Safety Agency, Yallambie, Australia

Background: National Diagnostic Reference Levels (NDRLs) have been developed in Australia for NM and Multi-Detector CT (MDCT), yet none have been released for the CT component of multimodality imaging. A survey of all Australian NM and PET facilities is underway in order to update the DRLs for nuclear medicine and to introduce NDRLs for CT scans conducted as part of multimodality procedures. The survey is being conducted as part of the NDRL Service (NDRLS).

Aim: To present early findings of analysis of the CT doses quoted in the SPECT/CT bone scan data submitted to the NDRLS Nuclear Medicine survey, including scan region frequency and dose distributions.

Method: During the first three months of the survey, dose information from over 1600 SPECT/CT bone scans had been submitted by 18 participants. These data were analysed to determine the most frequently scanned regions and the doses delivered during the most common scans. The distributions of multimodality CTs were then compared with those from the MDCT survey.

Conclusion: The CT doses delivered during SPECT/CT are, as expected, far smaller than those delivered in diagnostic CT departments. The differences in protocols and even nomenclature between different facilities in SPECT/CT bone scans make classification of scans into clearly defined body regions more complicated than for the case of MDCT. When future surveys are conducted of dose in multimodality imaging, it may be prudent to provide more guidance to participants relating to nomenclature. Furthermore, gathering additional information (such as $CTDI_{vol}$) might be beneficial.

P35
A FULLY INTEGRATED, COST-EFFECTIVE AND SOPHISTICATED CAPTURE SYSTEM FOR RADIOACTIVE GASES GENERATED DURING AUTOMATED RADIOPHARMACEUTICAL SYNTHESIS

D Stimson[1], A Pringle[1], D. Maillet[1], R Bhalla[1], T Venkatachalam[1], D Reutens[1]

[1]Centre for Advanced Imaging, The University of Queensland, Brisbane, Australia

Background: The demand for radiopharmaceuticals has increased due to the proliferation of PET both nationally and internationally. Increased production has led to a greater focus on stack monitoring with regulatory release limits for radioactive gases constantly under review. Various radioactive gas capture strategies have been employed including automated waste gas compression systems. Such systems however, may not be appropriate for use when flammable gases are used in radiopharmaceutical synthesis. Furthermore, the cost of gas compression systems can be prohibitively expensive.

Aims: To develop and implement a gas capture system for use with an automated [11C]carbon radiopharmaceutical synthesizer.

Methods:

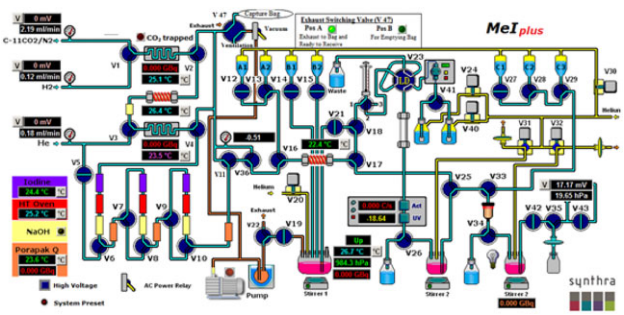


Figure 1 Graphical User Interface (GUI) of Synthra synthesizer depicting 4-port/2 way switching valve (V47)

A 4-port/2 way switching valve with position sensor was installed in the *Synthra MeI Plus* synthesizer. The synthesizer exhaust was connected to the switching valve so that gases are directed to a gas capture bag during cyclotron target transfer and during radiosynthesis. The synthesizer's vacuum pump with additional manual switch is used to empty the bag after the hot-cells radiation interlock allows operator access. The bag is fitted with a sensor arm to indicate the bag status. The valve position and bag status signals are sent to a microprocessor that is integrated with the Cyclotron Safety System. This prohibits the transfer of radioactive gas unless the bag is empty and the valve is in the correct position ('ready to receive'). A series of target transfers and radiosyntheses were conducted with the MediSmarts stack monitoring system used to detect any release of radioactive gas from the system.

© 2015 The Authors
Internal Medicine Journal © 2015 Royal Australasian College of Physicians

Results and Conclusion: A compact gas capture system was developed and implemented that is fully integrated with the cyclotron safety system. The gas capture system can be emptied without disconnection from the synthesizer. MediSmarts data demonstrate that the system is safe and effective.

P36
DESIGN, CONSTRUCTION & TESTING OF A TARGET CELL FOR IRRADIATION OF POWDERS USING A CYCLOTRON-GENERATED PROTON BEAM: APPLICATION TO TIO_2

S. Chan[1], D. Cryer[1], G. Griffiths[2], R.I. Price[1,3]

[1]Department of Medical Technology and Physics, Sir Charles Gairdner Hospital, Perth, Australia
[2]Australia Nuclear Science and Technology Organisation, Australia
[3]School of Physics, University of Western Australia, Perth, Australia

Background: Use of nanoparticles in typical consumer products has raised concern about their biological effects arising from cellular uptake. In support of in vivo research using a PET tracer, elucidating penetration of nanoparticles through the cell membrane, a custom chamber for irradiating powdered targets was designed to complement our existing semi-automated solid-targetry irradiation system mounted on an 18 MeV proton cyclotron.

Aims: Design, construct and test a target-chamber to contain dry aggregations of titanium dioxide nanoparticles (TiO_2-NP) for production of PET isotope ^{48}V ($t_{1/2}$ = 15.97 d) by proton-irradiation.

Methods: Dry, aggregated nanoparticle material is encapsulated in an aluminium holder with inner diameter 10 mm. Target-material is held in place with a thin aluminium window (thickness 25 μm), secured with double-sided tape and pressed in place with an annular aluminium cover (Figure). Overall dimensions of the powdered-target chamber are identical to our existing solid targetry-holder (diameter 25 mm; thickness 2 mm).

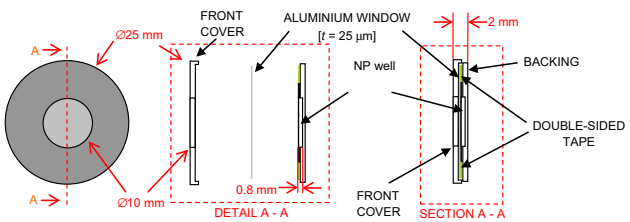


Figure Powder-target chamber schematic

The target-chamber is water-cooled on its back-surface (28 L/min; 18°C). Finite-element analysis (FEA) predicted its 3-D thermal profile under proton-irradiation, for target currents 1–20 μA at (degraded energy) 11.5 MeV. To examine the design, an empty target-chamber was irradiated for 30 min at 20 μA to confirm its integrity. Testing of the powder-filled chamber was conducted using pelletized TiO_2-NP as target-material, irradiated using 10 μA for 30 s. Several hours following EOB, calibrated cryo-HPGe γ-spectroscopy was performed on target to examine outcomes of possible reactions, particularly $^{48}Ti(p,x)$.

Results: FEA revealed that at 10 μA the target temperature was <100°C. Examination revealed no visible damage to the aluminium window or the chamber following 30 min of irradiation at 20 μA. γ-spectroscopy confirmed the overwhelming predominance of desired reaction $^{48}Ti(p,n)^{48}V$, in accord with deliberate restriction of primary-beam energy.

Conclusion: This study has demonstrated the design and preliminary testing of a powdered-target chamber for proton-irradiation (20 μA), generating up to 230 W of heat-flow. However, according to FEA the design has potential for higher currents. The entire irradiated target-chamber with its encapsulated material can be transported intact, directly to collaborating labs in order to minimise manual handling, radiation exposure and potential contamination of target material.

P37
LUTETIUM-177 DOTATATE PRODUCTION FOR NEUROENDOCRINE TUMOUR (NET) THERAPY WITH AUTOMATED RADIOPHARMACEUTICAL SYNTHESIS SYSTEM

A Aslani[1,2], GM Snowdon[1], D L Bailey[1,2,3], E A Bailey[1], P J Roach[1,2]

[1]Department of Nuclear Medicine, Royal North Shore Hospital, Sydney, Australia
[2]Sydney Medical School, University of Sydney, Sydney, Australia
[3]Faculty of Health Sciences, University of Sydney, Sydney, Australia

Introduction: NETs comprise a broad spectrum of different tumours which mainly originate from the gastroenteropancreatic tract. The fact that NETs express subtypes of somatostatin receptors, allows for diagnosis and treatmen t with somatostatin analogues. Peptide Receptor Radionuclide Therapy (PRRT) is increasingly be used to treat disseminated NETs. Radiolabelled somatostatin analogues, such as DOTATATE, now play an increasing role as second line therapy. The two most commonly used radioisotopes are yttrium-90 (^{90}Y) and lutetium-177 (^{177}Lu). Although the synthesis and purification of these radiopharmaceuticals can successfully be carried out manually in the laboratory, the use of automated synthesis systems is increasing. At our institution ^{177}Lu is used for PRRT of patients with well-differentiated NETs. The ^{177}Lu-DOTATATE (LuTATE) is synthesised in-house using an automated synthesis system. Here we report on our 18-month experience.

Methods: The Eckert & Ziegler Eurotope's Modular-Lab Pharm Tracer® automated synthesis system was utilised for the synthesis of LuTATE. All materials and methods used were followed as instructed or later modified by the manufacturer. In addition, the exact grades as well as the source of the reagents, peptide and $^{177}LuCl_3$ used were recommended by the manufacturer.

Results: Between August 2013 and December 2014, a total of 17 LuTATE syntheses were performed. A total of 13 patients (37 cycles) were treated. There were no failures associated with this system during this period. The average radiochemical purity (RCP) as determined by ITLC was above 99% (n = 17; 99.81 ± 0.05%) and above 97% (n = 3; 97.25 ± 1.47%) for HPLC (Figure 1).

Conclusions: The automated synthesis of LuTATE has proven to have a number of significant advantages over the manual method. In our one year experience the system has performed flawlessly delivering the required high-purity therapy doses.

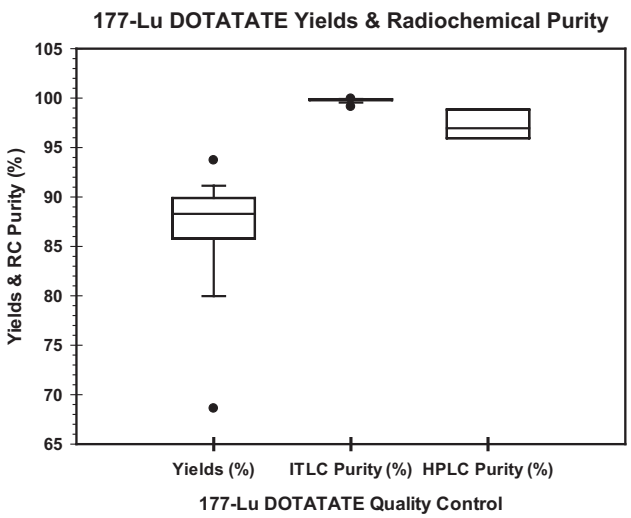


Figure 1 LuTATE yields and chemical purity

P38
OPTIMIZED PRODUCTION AND QUALITY CONTROL OF 68GA-DOTATATE FOR SMALL CLINICAL TRIALS

A Aghanejad[1], A R Jalilian[1], S Maus[2], H Yousefnia[1], S Moradkhani[1], M Pouladi[1]

[1]Nuclear Science and Technology Research Institute, Tehran, Iran
[2]Clinic of Nuclear Medicine, University Medical Centre Mainz, Mainz, Germany

Purpose: Optimized production and quality control of ^{68}Ga-DOTATATEas an efficient and preferable PET radiotracer for somatostatin receptor imaging

© 2015 The Authors
Internal Medicine Journal © 2015 Royal Australasian College of Physicians

in neuroendocrine tumors is of great interest. In these study efforts has been made to present a fast, efficient, cost-effective and facile protocol for ^{68}Ga-DOTATATE application in clinical trials.

Methods: ^{68}Ga-DOTATATEwas prepared using generator-based [^{68}Ga]$GaCl_3$ and DOTATATE at optimized conditions for time, temperature, ligand amount, gallium content and column purification using chromatographic methods followed by proper formulation. The biodistribution of the tracer in rats was studied using tissue counting and PET/CT imaging up to 120 min.

Results: ^{68}Ga-DOTATATE was prepared at optimized conditions in 7–10 min at 95°C followed by SPE using C_{18} cartridge (radiochemical purity ≈99 ± 0.88% ITLC, >99% HPLC, specific activity: 1280–2100 ± 5 GBq/mM). The biodistribution of the tracer demonstrated high kidney excretion of the tracer in 10–20 min consistent with reported water soluble peptide radiopharmaceuticals.

Conclusion: The whole production and quality control of ^{68}Ga-DOTATATE including labeling, purification, HPLC analysis, sterilization, LAL test) took 18–20 min with significant specific activity for administration to limited number of patients in a PET center.

P39
USE OF THE FLEXLAB RADIOSYNTHESISER FOR THE FULLY AUTOMATED SYNTHESIS OF 16B-[^{18}F]FLUORO-5A-DIHYDROTESTOSTERONE

H Tochon-Danguy[1], U Ackerman[1], S Poniger[2], G Chan[1], M. Morris[3], J Lewis[3], S Lyashchenko[3], A Scott[1,2]

[1]Molecular Imaging and Therapy, Austin Health, Melbourne, Australia
[2]Ludwig Institute for Cancer Research, Melbourne, Australia
[3]Memorial Sloan Kettering Cancer Center, New York, USA

Background: The increased interest in therapies directed at androgen receptors in metastatic lesions has sparked the development of PET tracers that can noninvasively image androgen receptor status across all lesions. The ^{18}F labeled 16β-[^{18}F]fluoro-5α-dihydrotestosterone (^{18}F-FDHT) analog has been identified as the most promising PET tracer for the imaging of the androgen receptor since it has the most favourable targeting properties for non-invasive imaging among AR-binding radiotracers studied to date.

Aims: In this study, we implement and evaluate the automated synthesis of ^{18}F-FDHT using a commercially available synthesizer in order to maximize amounts of radiotracer produced, improve reliability and reduce the radiation exposure to the operator.

Methods: We choose a FlexLab radiosynthesizer (IPHASE Technologies), which has been proven reliable for the radiolabeling of other complex molecules. To the dried mixture of K[^{18}F]F/kryptofix was added a solution of the triflate precursor (4 mg) and heated to 40°C for 15 min. The radiolabeled intermediates were then trapped on a SPE and after rinsing with water, transferred with 1.2 mL of ethanol to a second reactor. Reduction with 5 mg of solid NaBH4 was performed at 20°C for 7 min, followed by hydrolysis with 1.5 mL of 1M HCl at 80°C for 7 min. After hydrolysis, 1 mL of 1M NaOH was added and the crude reaction mixture purified via semi-preparative HPLC.

Results: Using $KHCO_3$ instead of K_2CO_3 as base resulted in higher yields and fewer side-products, which made HPLC purification of reaction intermediates unnecessary.

^{18}F-FDHT was produced in decay corrected radiochemical yields of 18–23% with a radiochemical purity >98% and a specific activity >55.5 GBq/μmol (1.5 Ci/μmol).

Conclusion: Using the FlexLab synthesizer ^{18}F-FDHT was produced without manual interventions, in 90 min, with sufficient quantities of the tracer for multiple doses ready for human injections.

P40
FULLY AUTOMATED PRODUCTION OF ZR-89 USING IBA NIRTA AND PINCTADA SYSTEMS

SS Poniger[1], HJ Tochon-Danguy[2], H Panopoulos[2], J Sachinidis[2], AM Scott[1,2]

[1]Ludwig Institute for Cancer Research, Melbourne, Australia
[2]Molecular Imaging and Therapy, Austin Health, Melbourne, Australia

Background: Few PET isotopes are suitable for antibody labelling since immunoPET requires that the isotope be attached to the mAb with high *in-vivo* stability and the decay half-life should match the pharmacokinetics of the mAb. Both ^{124}I ($t_{½}$ = 4.2 d) and ^{89}Zr ($t_{½}$ = 3.3 d) have a near ideal half-life for antibody-based imaging, but there are several advantages of using ^{89}Zr over ^{124}I.

Aims: Although ^{89}Zr is currently commercially available, its price is prohibitive for routine clinical applications for immuno-PET. The motivation for the present work was to fully automate the production of ^{89}Zr using commercially available systems.

Methods: The Nirta Solid Target from IBA was coupled to our 18/9 IBA cyclotron. Irradiations of the yttrium foils were performed on single 0.127 mm thick foils, double stacked 0.127 mm foils (~0.250 mm total) and 0.250 mm thick foils at beam energies of 14.9 MeV and 13.0 MeV. The irradiated target was loaded directly into the IBA Pinctada Metal module for dissolution & purification without disassembly. Purification of ^{89}Zr from ^{89}Y, ^{88}Y and other radionuclidic impurities was performed using a hydroxamate column, with ^{89}Zr eluted with 1.0 M oxalic acid.

Results: An average purified ^{89}Zr yield of 12.7 MBq (0.34 mCi)/μAh for 0.127 mm thick ^{89}Y-foils and 22.6 MBq (0.61 mCi)/μAh for 0.250 mm thick foils was achieved at 14.9 MeV. Gamma spectroscopy of the samples irradiated at 14.9 MeV showed low level of the radionuclidic impurity ^{88}Zr ($t_{½}$ = 83.4 d) at 393 keV, resulting from the (p,2n) reaction on ^{89}Y. Lowering the beam energy to 13.0 MeV eliminated the co-production of the ^{88}Zr impurity, but it also reduced the production yield of ^{89}Zr by ~30%.

Conclusion: The IBA Nirta Solid Target and Pinctada module are efficient and reliable automated systems for dissolution of the irradiated ^{89}Y target and purification/recovery of the ^{89}Zr PET radionuclide.

P41
F-18 RADIOLABELLING OF DBCO AS A SYNTHON FOR COPPER FREE CLICK CHEMISTRY USING THE FLEXLAB MODULE

U Ackermann[1], HJ Tochon-DAnguy[1], J Sachinidis[1], AM Scott[1]

[1]Austin Health, Melbourne, Australia

Background: Radiolabelling via the copper catalysed cycloaddition of alkynes and azides (click chemistry) has become a popular technique in recent years since it proceeds under mild reaction conditions and is compatible with a wide range of functional groups. When strained alkynes such as cyclooctynes are clicked with azides, copper (I) is not needed to promote this reaction. This copper free click chemistry is of particular interest in the radiolabelling of peptides and antibodies since they can be sensitive to copper ions.

Aims: The aim was to fully automate the synthesis of 4-[^{18}F]fluorobenzoyl DBCO and its coupling to azide bearing peptides using the FlexLab module.

Methods: To a dried K[^{18}F]F/kryptofix complex was added 5 mg (4-ethoxycarbonylphenyl) trimethylammonium triflate (20 μmol) in 0.5 mL of DMSO. Radiolabelling was performed at 110°C over 7 min in reactor 1. After that, 20 μL of 1 M aqueous tetramethylammonium hydroxide (20 μmol) in 4 mL acetonitrile were added for the hydrolysis of the intermediate ethyl 4-[^{18}F]fluorobenzoate. After evaporation of acetonitrile, two potential radiolabelling strategies of DBCO were investigated. The first strategy via [^{18}F]SFB and the formation of [^{18}F]FB-DBCO isolated via semi-preparative HPLC using a gradient elution technique. The second strategy 4-[^{18}F]fluorobenzoic acid and the formation of [^{18}F]FB-DBCO isolated via a semi-preparative HPLC using a gradient elution technique. The radioactive peak at 16.5 min was collected, trapped on a C-18 SPE cartridge and transferred to reactor 2 for subsequent copper free click chemistry labelling.

Results: Using the SFB-technique, [^{18}F]FB-DBCO was synthesised in 80 min with a decay corrected radiochemical yield of 28 ± 2%. Using the FB/DCC-technique, [^{18}F]FB-DBCO was synthesised in 70 min with a decay corrected radiochemical yield of 8 ± 2%.

Conclusion: Due to the higher yields of the [^{18}F]SFB method, this protocol is currently used to produce [^{18}F]FB-DBCO for copper free click labelling of azide bearing proteins.

P42
AUTOMATED SYSTEM FOR CLEANING AND FAST RESTARTING OF SYNTHESIZERS

G. Perkins[1], G. Pascali[1], I. Greguric[1], N. Paneras[1]

[1]ANSTO LifeSciences, Australian Nuclear Science and Technology Organisation, Sydney, Australia

© 2015 The Authors
Internal Medicine Journal © 2015 Royal Australasian College of Physicians

Background: Radiochemistry field is increasingly in high demand of flexibility and productivity. One of the most trivial and understated issues is represented by residual radioactive in the synthesis module, which slows down the preparation for next runs, especially with short half-life nuclides (e.g. 11C).

Aims: The aim of the project was to develop a system, that could be retro-fitted to the existing synthesis modules operated by ANSTO Life Sciences (Synthra GPextent and RNplus), allowing the operator to remotely refill and clean the apparatus using the existing software. Such a system is not yet commercially available.

Methods: We placed two Rheodyne valves to operate back-to-back in order to route solvents and helium push. By using a combination of tubing lengths, timed control and flow detectors, we programmed a sequence of events using an Arduino platform to deliver the cleaning solvents. Execution of this complete cleaning sequence is triggered through the Synthra software.

Results: We were able to accurately dispense 1 mL ± 10% (using ethanol, water and acetone) across up to 22 different vials, allowing any Synthra brand module to be utilized. We employed the minimum amount of moving parts and it flawlessly interfaced the original software.

Conclusion: The team in ANSTO Life Sciences has designed and built two generations of cleaning systems that can be retro-fitted to the Synthra brand modules. This apparatus has allowed a 30% increase in production of 11C tracers at the facility. This concept is easily expandable and could be incorporated as a standard feature in next generation synthesis modules.

P43
ARE TURN-KEY RADIOPHARMACEUTICALS TROUBLE FREE?

S Taylor[1]

[1]*Department of Nuclear Medicine, Royal Brisbane and Women's Hospital, Brisbane, Australia*

Background: In 2014 Nuclear Medicine, RBWH was awarded at TGA license for the manufacture and distribution of multidose vials of [^{18}F]FDG and the manufacture and sale of the API [^{18}F]F-18. We also purchased FASTlab chemistry modules and commenced the work up of FDG for clinical use and distribution, using commercially available FDG cassettes.

Aims: To demonstrate that FDG stabilised with sodium thiosulfate and/or ethanol and manufactured on FASTlab chemistry modules using commercially available FDG cassettes satisfies the requirements of our TGA license.

Methods: Pre-clinical FDG, stabilised with sodium thiosulfate and/or ethanol, was produced in commercially available citrate and phosphate buffered formulations with activities in excess of 500 GBq. Yield and quality were assessed at EOS to demonstrate the product satisfied the BP monograph for FDG. Radiochemical purity and visual clarity were determined at 4 and 16+ hours post-EOS to demonstrate the product was suitable for use at its 16 h expiry time.

Results: Initial results obtained with both citrate and phosphate cassettes produced FDG that passed our QC criteria, and possessed RCP >95% at expiry. Initial reactions with citrate cassettes afforded yields of ~35%*. Product obtained with phosphate cassettes was uniformly observed to contain particulates** prior to the expiry time. Attempts to suppress particulate formation were unsuccessful. Citrate cassettes with a manufacture date post-September 2014 were found to be suitable for clinical use.

Formulation	N	RCY	RCP (%)			Endotoxin	Sterile	Clarity		
		(%)	T_0	T_4	T_{16}	EU/mL		T_0	T_4	T_{16}
Initial Citrate	5	35*	>98	>96	>96	<0.5	Yes	Clear	Clear	Clear
Phosphate	7	68	>98	>96	>96	<0.5	Yes	Clear	Cloudy**	Particles**
Citrate	5	64	>98	>96	>96	<0.5	Yes	Clear	Clear	Clear

Conclusion: The clinical implementation of commercially available radiopharmaceuticals is not immune to problems. A bad batch of SPE cartridges, or the formation of particulates in the product, while random, demonstrates the need to carefully examine the product prior to clinical use.

P44
RADIOSYNTHESIS AND QUALITY CONTROL OF ^{68}GA-DFO-UBI 29–41

W Hsieh[1], *M Ali*[1], *D Smyth*[1], *C Tsopelas*[1]

[1]*RAH Radiopharmacy, Nuclear Medicine Department, Royal Adelaide Hospital, Adelaide, Australia*

Background: Ubiquicidin (UBI) 29–41 is an antimicrobial peptide with known high specificity for bacterial cell membrane, and this property has the potential to discriminate an infectious lesion from inflammation *in vivo*. This peptide was previously labelled with ^{99m}Tc via the HYNIC conjugating group, and ^{68}Ga via the NOTA group. In this study we examined the desferrioxamine (DFO)-UBI 29–41 reaction with ^{68}Ga.

Aims: The aim of this study was to determine the conditions to achieve successful radiosynthesis and quality control assessment of ^{68}Ga-DFO-UBI.

Methods: ^{68}Ga-chloride was eluted from a ^{68}Ge/^{68}Ga generator (IGG-100; Eckert & Ziegler) with 0.1 M HCl onto a SCX cartridge. ^{68}Ga-chloride was eluted with acidified sodium chloride into the reaction vial (~250 MBq, 0.5 mL). Radiosynthesis was performed (n = 3) at room temperature for 20 minutes in the presence of acetate buffer (pH 4, 0.2 mL), DFO-UBI (100 μg) and [1:11] ethanol : water (1 mL) in a nitrogen vial. At completion, the crude product was assessed by ITLC-SG paper developed with NH_4OAc (77 g/L) in [1:1] MeOH : water, and then the strip was scan-analysed (Scan-RAM; LabLogic). The product was purified by filtration (0.02 μm filter, Whatman) using [1:1] EtOH : saline. Product was analysed by HPLC (Shimadzu) using a C18 column/solvent gradient mixture of 5–100% acetonitrile in water (+0.1% TFA). Radiotracer integrity was tested by HPLC at room temperature at 2 hours post-radiosynthesis.

Results: ITLC gave crude product (R_f = 0.8) in 83 ± 2% radiochemical yield. Using the fine filter, ^{68}Ga-hydroxides were exclusively removed to give ^{68}Ga-DFO-UBI (R_T = 7.4 min) with 98 ± 2% radiochemical purity and 0.5 ± 0.1% $^{68}Ga^{3+}$ ions (R_T = 1.5 min). The radioactive product was stable after 2 hours (RCP was >95%).

Conclusion: ^{68}Ga-DFO-UBI 29–41 was conveniently synthesised and purified in 25 minutes, to give a useable product with high radiochemical purity. We are currently exploring the potential of this radiotracer as an infection imaging agent in pre-clinical studies.

P45
TITANIUM-45 AS A CANDIDATE FOR PET IMAGING: CYCLOTRON-BASED PRODUCTION & HYDROXYLAMINE-FUNCTIONALIZED RESIN SEPARATION & PURIFICATION

R.I. Price[1,2], *R.W. Sheil*[1,3], *R.K. Scharli*[1,2], *S. Chan*[1], *P. Gibbons*[1], *C. Jeffery*[1], *L. Morandeau*[1]

[1]*Radiopharmaceutical Production & Development (RAPID) Laboratory, Medical Technology and Physics, Sir Charles Gairdner Hospital, Perth, Australia*
[2]*School of Physics, University of Western Australia, Perth, Australia*
[3]*Imaging & Applied Physics, Curtin University, Perth, Australia*

Background: Transferrin (TF) and its receptor TFR1 mediate recruitment by cancer cells of factors for their multiplication, adhesion, invasion and metastatic potential. Apo-TF can bind Titanium(IV) more avidly than it does iron. Indeed, Fe(C-lobe)Ti(N-lobe)-TF may mediate Ti cellular entry via TFR1. Thus, the PET-tracer isotope ^{45}Ti ($T_{1/2}$ = 3.08 hr; β^+-ratio = 85%; mean β^+-energy = 439 keV) may elucidate biomechanisms involving TF-binding and internalisation.

Aim: Produce high-purity no-carrier-added ^{45}Ti at sufficient activity/specific-activity for imaging.

Method: ^{45}Ti was produced using ^{45}Sc(p,n)^{45}Ti reaction by irradiating 100-μm thick scandium discs at 11.6 MeV using an 18 MeV cyclotron. This degraded beam-energy abolishes 'contaminating' reactions ^{45}Sc(p, n + p)^{44}Sc and ^{45}Sc(p,2n)^{44}Ti. Separation of Ti (mainly from Sc) and its purification was achieved with hydroxylamine hydrochloride-functionalised resin. Disc dissolved in 2 mL 6 M HCl, then diluted to 2 M. Eluted through column to waste-fraction-1 (w1 – Fig.). Then 6 mL 2 M HCl eluted through column to w2, followed by 6 mL traceSELECT H_20 to w3. Finally, Ti eluted into successive 1 mL product-fractions (p1–4) using 5 mL 1 M oxalic acid; (total ~1 hr). ^{45}Ti measured using γ-spectroscopy. Sc in the same vials determined using ICP-MS.

© 2015 The Authors
Internal Medicine Journal © 2015 Royal Australasian College of Physicians

Results: Typical production (40 μA; 60 min) yielded 1.8 GBq, EOB. Radionuclidic analysis revealed ^{44}Sc (<0.19%) as only contaminant. Typical separation shown in Figure; only 30% of original activity of 45Ti (EOB-corrected) was in product, with vial of highest activity (p1) containing 14%.

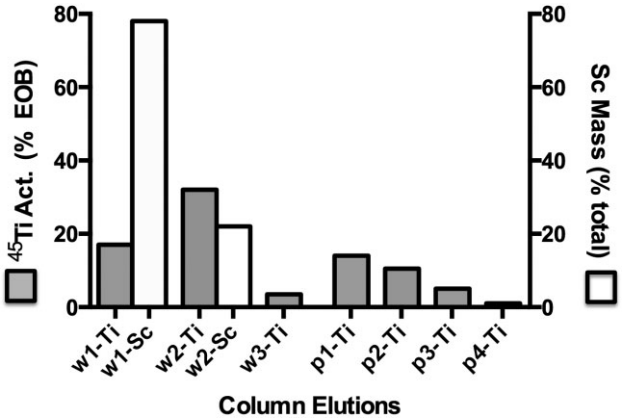


Figure ^{45}Ti activity from calibrated γ-spectroscopy, as percent of total ^{45}Ti EOB activity. Elution fractions w1-Ti to w3-Ti were waste. Elutions p1-Ti to p4-Ti were product, each 1 mL. Elution-profile for (cold) Sc mass (ICP-MS) also shown, with negligible total in p-fractions (<0.017%)

Conclusions: Despite ^{45}Ti loss into waste (total 53%, EOB-corrected), ^{45}Ti of acceptable specific activity and radionuclidic purity was produced from ^{45}Sc(p,n)^{45}Ti, with separation/purification by hydroxamate-column chemistry. Two 0.100-μm thick Sc target-discs yield isotope of adequate activity without need for concentration, for subsequent radiolabelling and preclinical imaging.

P46
FREQUENCY OF SYMPTOMATIC GASTROPARESIS (SG) POST-LUNG TRANSPLANTATION (LTX)

G Ramaseshan[1], K Yap[1], M Cherk[1], D McGiffin[3], G Snell[2], V Kalff[1]

[1]Department of Nuclear Medicine, The Alfred Hospital, Melbourne, Australia[2]Lung Transplant Unit, The Alfred Hospital, Melbourne, Australia[3]Department of Cardiothoracic Surgery, The Alfred Hospital Melbourne, Australia

Background: SG is an important issue that affects recovery and quality of life post-LTx.

Aims: The aim of this retrospective study was to determine frequency of gastroparesis, duration and possible associations.

Methods: Over 2 years, 136 LTx were performed, of which 42 had a gastric emptying study (GES) using a standardized radiolabelled semisolid meal with gastroparesis defined as gastric emptying half-time (GEt/2) >150 min. The patients medical records were retrospectively reviewed, data expressed as mean ± SD and analysis was performed using 2 way Fisher exact and unpaired tests.

Results:

		Gastroparesis	No Gastroparesis
LTx indications (Patient number)	COPD	9	9
	Cystic fibrosis	3	7
	Interstitial lung disease	0	7
	Other pathologies	3	4
Diabetes (Patient number, %)		7/15 (47%)	15/27 (55%)
Presence of prokinetic agents (Patient number, %)		6/15 (38%)	9/27 (33%)
Presence of calcineurin inhibitors (Patient number, %)		15/15 (100%)	26/27 (95%)
Clamshell approach (Patient number, %)		10/25 (40%)*	15/25
Bilateral anterior thoracotomy approach (Patient number, %)		5/17 (29%)*	12/17
Average duration of operation		7.1 ± 2.4 hrs (duration not available in 2 patients)	6.5 ± 1.6 hrs (duration not available in 2 patients)

* p = 0.53

Gastroparesis was present in 15/42 patients, including 10 with GEt/2 too abnormal to calculate. In all patients with gastroparesis, GES was performed <110 days post-LTx. 0/2 single lung transplants had gastroparesis. All 42 patients undergoing GES had upper gastrointestinal symptoms compared to 16/94 who did not undergo GES ($p < 0.001$). In the 15 patients with gastroparesis, symptoms resolved in 9 (including 5 with change in medications only), 12 and 13 patients by 3, 6 and >12 months post-GES respectively. Two patients remained symptomatic beyond 1 year.

Conclusion: In LTx patients who had upper GI symptoms and underwent GES, gastroparesis was objectively demonstrated in 36% of patients. Symptoms tended to improve by 3 months. No definite readily explainable association was found in this study.

P47
LUTETIUM THERAPY – A REVIEW OF PATIENT RESPONSES TO PRRT AT THE QUEEN ELIZABETH HOSPITAL

J Lawrie[1], M Kitchener[1]

[1]The Queen Elizabeth Hospital, Adelaide, Australia

Background: The Queen Elizabeth Hospital Peptide Receptor Radionuclide Therapy (PRRT) service using Lutetium-177 (^{177}Lu) Octreotate for patients with progressive, metastatic Neuroendocrine tumours) has now been in operation for 4 years. Since our early review 46 patients have entered the programme and commenced/completed an induction course of therapy. 13 patients have received maintenance therapy. The aim is to confirm whether our early success is continued with a larger patient cohort and highlight the ongoing benefit of therapy.

Method: Review of patient responses to therapy using both objective and subjective parameters expanding on the information presented at the end of our first year and including data on time to progression following therapy. Parameters evaluated include radiological changes, biochemical markers and symptomatic response, as evaluated by EORTC QOL C30 Quality Of Life (QOL) questionnaire.

Results: All patients accepted for treatment had confirmed high-level avidity on baseline Somatostatin Receptor (SSR) scintigraphy. Baseline staging included structural imaging and Chromogranin A (CgA) measurements. All patients completed a baseline QOL questionnaire, with additional questionnaires completed at the end of cycles. A comparison was made between pre- and post-PRRT for these parameters, as well as time until disease progressed. Over 90% of patients derived benefit from therapy as indicated by improvement in at least two of the parameters reviewed. 85% of patients did not require additional PRRT therapy for over 12 months with 30% still clinically well without further PRRT, 24 months after completing their induction therapy.

Conclusion: Neuroendocrine tumours are known to be radiosensitive and respond well to PRRT. Our results demonstrate clinical benefit, with a combination of improved QOL indices, symptom control, biochemical and radiological response. The length of time until disease progression requiring further PRRT in the majority of our patients indicates that PRRT provides a long-term benefit to these patients.

P48
RE-TREATMENT RATES AFTER LOW-DOSE RADIOACTIVE IODINE ABLATION FOR LOW-RISK PATIENTS WITH THYROID CANCER

E Clingan[1], S Beuzeville[1], R Quinn[1], R Nour[1]

[1]The St George Hospital, Kogarah, Australia

Background: In early 2012, several papers were published supporting the role of low dose (1.1 GBq) post-thyroidectomy radio-iodine (RAI) ablation

© 2015 The Authors
Internal Medicine Journal © 2015 Royal Australasian College of Physicians

in low risk thyroid cancer patients. Our institution adopted this treatment strategy for patients with low risk thyroid cancer in July 2012. Prior to that time all post-thyroidectomy patients with cancer were treated with high dose radio-iodine (4 GBq).

Aims: To examine re-treatment rates in low risk thyroid cancer patients treated with low dose RAI compared to the re-treatment rates prior to the institution of this policy.

Methods: A retrospective audit was performed of the Radiology Information Systems and a departmental database of all RAI therapies that commenced in the period July 2007 to July 2014. Patient demographics, pathology, administered dose of RAI, stimulated serum thyroglobulin & thyroglobulin antibodies (following ablation and at follow-up); and results of surveillance (stimulated thyroglobulin and diagnostic whole body scans) studies were documented.

Results: 45 patients received 49 low-dose RAI therapies, of which 4 of the 45 treated patients required re-treatment, giving a re-treatment rate of 8.8%. 380 patients received 456 high-dose RAI therapies of which 49 of the 380 treated patients required re-treatment, giving a re-treatment rate of 12.9%. Similar characteristics were present in both re-treatment groups except for baseline and surveillance thyroglobulin levels (Table).

Characteristics of Patients Requiring Re-treatment	High-Dose RAI	Low-Dose RAI
Average Age	49.6	48.7
% Female	73	100
% Papillary Thyroid Carcinoma	81.60	100
Median TUMOUR SIZE (mm)	22	22.5
Median Baseline Thyroglobulin (μg/L)	8	2.15
Median Surveillance Thyroglobulin (μg/L)	0	1.65
% Positive RAI Scan at Surveillance	81	100

Conclusion: This study demonstrates the institution of low dose RAI ablation post-thyroidectomy for patients with low risk thyroid cancer did not appear to adversely impact on re-treatment rates.

P49
SEVERE PULMONARY OEDEMA: DEMONSTRATED ON V/Q SPECT

L Renshaw[1]

[1]*Hunter New England Imaging, New Lambton Heights, Australia*

Background: V/Q SPECT imaging is well established in the diagnosis of pulmonary embolism. Other pulmonary diseases can often be demonstrated and of high clinical importance to treating physicians.

Aims: A case study of severe pulmonary oedema; demonstrated on a V/Q SPECT scan.

Methods: A 56 year old male inpatient was referred from the Coronary Care Unit for a VQ scan. The patient had background of a recent ST Segment Elevation Myocardial Infarction with Hospital acquired pneumonia (HAP) and had been previously in intensive care for a worsening of his fevers and haemoptysis. Once stable the patient had been transferred to the Coronary Care Ward and was placed on IV antibiotics to cover for the HAP. The patients X-rays had shown some patchy consolidation presumed to be alveolar oedema.

Results: The Ventilation and Perfusion Images both showed a general peripheral lung distribution of tracer, with photopaenia in the central lung aspects. A SPECT/CT of the perfusion phase showed central lobular fluid/consolidation consistent with severe pulmonary oedema.

Conclusion: Although the treating team of the patient knew of some pulmonary oedema, the team were still unsure of the main condition causing the patients sudden decline. They had questioned PE, HAP and infection all as causes. The V/Q scan unveiled the extent of the patients pulmonary oedema and led to the team changing the treatment for the patient. The patient was placed on oral steroids which subsequently resolved his oedema.

P50
INCIDENTAL FINDING OF BREAST LESION ONTC-99M MIBI MYOCARDIAL PERFUSION IMAGING

L Renshaw[1]

[1]*Hunter New England Imaging, New Lambton Heights, Australia*

Background: Tc-99m methoxyisobutylisonitrile (MIBI) is a well established radiotracer used in Myocardial Perfusion imaging. Tc-99m MIBI is also a known oncotropic tracer which gives rise to the possibility of extracardiac incidental findings on studies which may hold high clinical significance for patients presenting for this study.

Aims: Case study of an incidental finding of a breast lesion on Tc-99m MIBI Myocardial Perfusion Imaging.

Methods: A 62 yr old female presented for investigation of ischaemic heart disease, with high risk factors. A myocardial perfusion scan was performed as per departmental protocol, with results showing no scan evidence of impaired coronary flow reserve and no scan evidence of myocardial scar. Noted in the imaging was an accumulation of tracer within the left breast which the reporting physician reported as being highly suspicious for breast cancer. A SPECT/CT was performed to localise the lesion to confirm its presence.

Results: The incidental lesion was noted in the patients report and correlation imaging was suggested. The patient went on to have further investigations which proved the lesion to be positive for a Grade 2 Invasive Ductal Carcinoma. The patient went on to have a lumpectomy of the lesion, and 2 lymph nodes removed which were negative.

Conclusion: This case highlights the clinical importance of incidental findings in Tc-99m MIBI Imaging. SPECT/CT can prove to be helpful when highlighting noncardiac findings in Myocardial Imaging.

P51
BONE SCINTIGRAPHY IN THE EVALUATION OF ACUTE MASTOIDITIS IN A CONFUSED PATIENT

J Behn[1], *QL Chiam*[1], *R Alipour*[1], *H Dixson*[1], *K Lee*[1]

[1]*Bankstown Hospital, Sydney, Australia*

Clinical history: 78 year old afebrile diabetic female with Alzheimer's disease presented with 1 week history of increasing confusion and generalised weakness on a background of recurrent falls for last month. There were no relevant findings on examination. Laboratory results revealed a raised white cell count and inflammatory markers. Non-contrast CT brain demonstrated inflammatory changes in the left mastoid, left middle ear and paranasal sinuses. CT of the chest, abdomen and pelvis demonstrated no source of infection. The treating team was not convinced that the source of infection was due to left otomastoiditis and acute sinusitis and subsequently requested a bone scan.

Findings: The bone scan with SPECT-CT demonstrated marked delayed uptake with no hyperaemia, bony erosion or destruction in the left mastoid, consistent with acute left mastoiditis without evidence of complicating osteomyelitis. There were also recent sacral and ribs fractures on the bone scan. A contrast enhanced CT brain to assess for complications of mastoiditis was suggested. No dural sinus thrombosis, intracranial abscess, or subperiosteal abscess was evident. Intravenous followed by oral antibiotics were administered with the patient returning to her pre-morbid state.

Discussion: Acute mastoiditis is a suppurative infection of the mastoid air cells and a potential complication of acute otitis media. In acute otitis media, some mastoid inflammation can be seen as the mastoid air cells and middle ear cavity are contiguous and share the same modified respiratory epithelium. Inflammation of the bony periosteum can induce abnormal new bone growth (explains mastoid uptake on bone scan) and is frequently seen as a result of acute or chronic infection.

Conclusion: Acute mastoiditis is usually clinically apparent but in mentally compromised individuals, this can be challenging to diagnose. The bone scan assisted in supporting the diagnosis of left mastoiditis which initiated appropriate treatment and prevented serious suppurative complications.

P52
HYPERCALCEMIA AND ITS EFFECT ON THE BIODISTRIBUTION OF ^{99M}TECHNETIUM-HYDROXYMETHYLENE DIPHOSPHONATE (^{99M}TC-HDP) IN SKELETAL SCINTIGRAPHY: A CASE STUDY

B Robinson[1], *L Baker*[1]

[1]*The Royal Brisbane and Women's Hospital, Brisbane, Australia*

Background: Hypercalcemia is a relatively common disorder which may be attributed to conditions including hyperparathyroidism, tuberculosis, sarcoidosis, as well as a number of malignancies. Patients may be asymptomatic until serum calcium levels exceed 11 mg/dl, after which they may

© 2015 The Authors
Internal Medicine Journal © 2015 Royal Australasian College of Physicians

experience symptoms such as hypertension, nausea, vomiting, lethargy, renal calculi or skeletal pain.

Aim: To follow the clinical case of a 71-year-old Caucasian male who has hypercalcemia and explores the condition's effect on the biodistribution of (^{99m}Tc-HDP) on a skeletal scintigram.

Method: As per the Royal Brisbane and Women's Hospital's protocol, the patient's scan was conducted with flow, blood pool and delayed imaging. The reporting physician requested that a SPECT/CT scan also be performed to enhance anatomic localisation of an abnormal focus of uptake observed within the upper gastrointestinal tract. Kit reconstitution of ^{99m}Tc-HDP was immediately reviewed and found to have been within acceptable limits. Using a variety of resources, the biodistribution of ^{99m}Tc-HDP was then examined, followed by a subsequent review of the disease process of hypercalcemia.

Results: The patient's delayed images depicted atypical biodistribution of ^{99m}Tc-HDP, with a region of unexpected extra-osseous uptake confined within the stomach. As the quality control of the ^{99m}Tc-HDP kit was deemed sufficient, the patient's clinical history was then considered Consequently, the reporting physician concluded that the abnormal radiotracer distribution was directly related to the patient's hypercalcemia.

Conclusion: Upon observation of unusual 99mTc-HDP biodistribution, the radiopharmaceutical kit's QC results and labelling efficiency should first be confirmed. In instances where QC results are satisfactory, other explanations should be sought. There are a number of disease processes that may cause extraskeletal uptake such as myocardial infarction and calcification of blood vessels and as this clinical example illustrates, hypercalcemia. This case study highlights the importance of understanding factors that may contribute to altered biodistribution in Nuclear Medicine studies.

P53
A RARE CASE OF METASTATIC PAPILLARY THYROID CANCER TO THE BREAST AND OTHER SOFT TISSUES

C Prajogo[1], A Mazar-Atabaki[1], R Mansberg[1,2], R Russo[1,2]

[1]Department of Nuclear Medicine, Concord Hospital, Concord, Australia
[2]Sydney Medical School, University of Sydney, Sydney, Australia

Background: Papillary Thyroid Cancer (PTC) is the most common thyroid malignancy, and is generally associated with good prognosis. The presence of metastases is associated with poorer prognosis. Common sites of metastases are lung and bone with other sites such as soft tissue and liver being extremely rare. Metastatic disease to the breast is exceedingly rare.

Aims: To assess the patient's case study of PTC with rare metastasis to the breast.

Method: A 78-year-old female was referred for an I-131 ablation for recurrent thyroid cancer. The whole body scan that was performed demonstrated marked right breast uptake as well as multiple soft tissue, lung and skeletal metastases. She was referred for a FDG-PET scan for further investigation which showed moderate uptake in the right breast and other sites. A breast biopsy was performed and confirmed PTC.

Results: The I-131 scan demonstrated iodine avid tissue in the right breast, left paraspinal musculature, the upper and lower lobes of the right lung, soft tissue subcutaneous masses in the midline of the upper abdomen, left lower abdomen, right gluteal soft tissues, faint uptake in the right upper medial thigh and left upper calf with a destructive lesion in the L4 pedicle, which all demonstrated mild and less extensive FDG uptake in the FDG-PET scan.

Conclusion: In differentiated PTC, this case reconfirms the benefits of I-131 total body scanning over FDG-PET, and highlights that papillary thyroid cancer can metastasise to sites such as breast and soft tissue, albeit rarely. Furthermore, histological confirmation should nevertheless be performed to exclude primary cancer from metastatic PTC.

P54
TAKOTSUBO CARDIOMYOPATHY: AN INCIDENTAL DIAGNOSIS ON GATED MYOCARDIAL PERFUSION SPECT

A Iravani[1], C Hercus[1], N Loh[1]

[1]Department of Nuclear Medicine and WA PET Service, Sir Charles Gairdner Hospital, Perth, Australia

Background: Takotsubo Cardiomyopathy (TCM) or stress-induced cardiomyopathy is characterized by the transient apical ballooning during systole in the absence of significant epicardial coronary artery disease. The clinical presentation is usually indistinguishable from that of acute coronary syndrome (ACS) and often preceded by a stressful event. Transthoracic echocardiography (TTE) provides a quick method of diagnosing wall motion abnormalities typically seen in TCM, which extend beyond the distribution of any single coronary artery. The diagnosis of TCM is typically confirmed with cardiac angiography (CA). There are only few reported cases of TCM, primarily suspected or retrospectively diagnosed by gated myocardial perfusion SPECT (GSPECT) especially in an asymptomatic patient.

Aims: (1) To illustrate the typical perfusion and wall motion abnormalities in TCM on GSPECT and (2) to underscore the importance of differentiating TCM from ACS.

Methods and Results: A 62-year-old female, with newly diagnosed acute myeloid leukaemia, referred for assessment of the baseline left ventricular ejection fraction (LVEF) with GSPECT, prior to the commencement of chemotherapy with anthracyclines. There were neither significant cardiac risk factors nor preceding cardiac symptoms. Perfusion SPECT images demonstrated defects in the peri-apical segments. Gated cinematic display showed apical/periapical akinesis and ballooning with moderately impaired LVEF (36%). TTE showed similar pattern of wall motion abnormalities, characteristic of TCM. CA did not reveal significant coronary atherosclerosis. Anthracycline was withheld from the chemotherapy regimen. Follow-up TTE 45 days later demonstrated interval resolution of apical ballooning and normalization of LVEF.

Conclusions: This case depicts incidental findings characteristic of TCM on GSPECT in the absence of cardiac symptoms. The knowledge of the scintigraphic findings in TCM will enable differentiating this unique cardiomyopathy from ACS. The importance of considering this diagnosis is punctuated by the diverging outcomes, with very low in-hospital mortality (1–2%), and the implications on clinical management of the two diagnoses.

P55
FLUORO-DEOXY-GLUCOSE POSITRON EMISSION TOMOGRAPHY DIAGNOSED SMALL BOWEL INTUSSUSCEPTION DUE TO HODGKINS LYMPHOMA

A Garg[1], P Sullivan[1], A Lockhart[1]

[1]Medical Imaging, The Canberra Hospital, Canberra, Australia

Abstract: 53 year old man with human immunodeficiency virus (HIV) developed 3–4 weeks of severe crampy abdominal pain and nausea. The patient had been started on anti-retroviral therapy only 6 months prior. Computed tomography (CT) scan of the abdomen and pelvis demonstrated lymphadenopathy which was considered suspicious for lymphoma. Fluorodeoxy-glucose Positron Emission Tomography (FDG PET/CT) was performed which demonstrated FDG avid disease above and below the diaphragms. The low dose CT also demonstrated the presence of 'fat in bowel sign' with an associated nearby FDG avid mass suggesting a small bowel intussusception. Subsequent Diagnostic CT was co-registered better demonstrating the intussusception without vascular compromise. The patient subsequently underwent a laparotomy. At laparotomy the intussusception was identified and manually reduced. The involved segment of small bowel was resected and sent for surgical pathology. The macroscopic pathological specimen demonstrated an endoluminal mass measuring up to 3.5 cm with a yellow/fleshy dimpled surface. Histologically the lesion was Classical Mixed Cellularity Hodgkin lymphoma. On immmuno-histochemistry the tumour showed diffuse/strong nuclear positive Ebstein Barr Virus-encoded RNA staining. This is the first case we have identified in the literature of a FDGPET-CT diagnosed small bowel intussusception due to lead point of a Classical Hodgkins lymphoma tumour mass in an adult.

P56
A V/Q SCAN LEADING TO THE DIAGNOSIS OF A BRONCHIAL NEUROENDOCRINE (ATYPICAL CARCINOID) TUMOUR

R Garzan[1], A Aminazad[1], M Jost[1], F Thien[1]

[1]Eastern Health, Melbourne, Australia

Background: Apart from the diagnosis of Pulmonary Embolism, V/Q scans can be helpful in establishing alternative diagnoses.

Aims: We describe a 59-year-old man whose abnormal V/Q scan led to the final diagnosis of a bronchial Neuroendocrine tumour.

Methods: A 59-year old man (life-long non-smoker) presented to the emergency department with several weeks of dyspnea and chest infection

© 2015 The Authors
Internal Medicine Journal © 2015 Royal Australasian College of Physicians

for several months and calf tenderness. His other history included poorly controlled diabetes mellitus type 2 and a left below knee amputation and cataract surgery. He initially had a chest Xray, which showed some streaky changes behind the heart shadow, but otherwise no parenchymal lung abnormality. He subsequently had a V/Q scan, then a CT scan of chest, bronchoscopy with biopsy and then an In-111 Octreotide scan.

Results: The V/Q scan demonstrated severely diffused reduction of ventilation and perfusion (matched) to the left lung. The CT scan of the chest showed an infiltrating soft tissue mass in the distal left main bronchus extending into and obliterating the bronchus to the left lower lobe. The bronchoscopy confirmed the left main bronchus tumour, which was biopsied. The biopsy was consistent with a neuroendocrine (atypical carcinoid) tumour (Grade 2). He subsequently had an In-111 Octreotode scan for staging, which showed uptake in the tumour and a further focus of uptake in the left mid to upper zone of the left lung, but no extra pulmonary metastasis. The patient wsubsequently managed with a left pneumonectomy.

P57
INCIDENTAL FINDING OF A LARGE OVARIAN CYST ON A WHOLE BODY BONE SCAN

S Fischer[1], G Larcos[1,2], G Minch[1], R Dickinson[1], P Monaghan[1]

[1]Southern Nuclear Imaging Group, Batemans Bay, Australia
[2]Westmead Hospital, Sydney, Australia

Background: A 71 year old female presented to the Nuclear Medicine Department for the investigation of chronic intermittent left hip pain which had deteriorated in the last 6 months. The patient had a history of previous left total arthroplasty (9 years ago). The study was requested to assess for loosening, infection or trochanteric bursitis.

Methods: The patient was injected with 1000 MBq of 99mTc-HDP immediately followed by dynamic flow and blood pool images of the Lumbar spine and pelvis. The patient returned later for a delayed whole body bone scan with lateral skull views and a SPECT/CT of the pelvis/femora.

Results: Flow and blood pool images show a large vascular mass in the pelvic area and no hyperaemia in the proximal left femur. On the delayed images there is subtle diffuse uptake within the pelvis, superior to the urinary bladder. SPECT/CT confirmed that this uptake corresponded to a large soft tissue mass extending toward the umbilicus; its origin could not be clearly identified, but was thought to be either uterine or ovarian. The scan appearance in the periprosthetic bone of the left acetabulum and proximal left femur were suggestive of possible early loosening. Following the bone scan, formal radiological correlation of the pelvis confirmed a 15–16 cm mass within the pelvis; not entirely specific, but thought to be due to a large fibroid uterus. Surgical correlation was then performed and revealed a large ovarian cyst weighing a total of 1.6 kg. Following the removal of the ovarian cyst the patient's symptoms fully resolved.

Take home lessons: concurrent low dose CT can demonstrate alternative causes of pain; low grade uptake can be demonstrated in soft tissue pelvic tumours; to the uninitiated, the hypervascularity in the pelvis midline can be confused with the urinary bladder, however a normal bladder should not be seen so soon.

P58
DISAPPEARING BONE DISEASE (GORHAM'S DISEASE) DEMONSTRATED ON SPECT/CT IMAGING

A Mazar-Atabaki[1], A Russon [2], K Sesel[2], R Mansberg[1,2]

[1]Department of Nuclear Medicine, Concord Hospital, Concord, Australia
[2]Sydney Xray, Bondi Junction, Australia

Background: Gorham's disease (vanishing bone disease) is a very rare skeletal condition of uncertain aetiology, characterised by the uncontrolled proliferation of distended, thin walled vascular or lymphatic channels within bone, which leads to resorption and replacement of bone with angiomas and/or fibrosis.

Aims: to assess the patient case study of a lytic bone lesion due to a rare diagnosis of 'vanishing bone disease' (Gorham's disease).

Methods: A 55-year-old male with nonspecific headache was referred for a CT scan, which demonstrated a lytic lesion in the left parietal skull. A Bone SPECT/CT and MRI were performed to further evaluate the lesion and assess for the presence of occult lesions elsewhere in the skeleton and reviewed by nuclear medicine physician/radiologist to assess for the presence of malignancy.

Results: The imaging investigations revealed a large solitary lytic lesion in the left parietal bone with pseudo-herniation of the brain into the defect. No other occult lesion was demonstrated elsewhere in the skeleton. The patient subsequently underwent left parietal craniectomy, reduction of encephalocoele and reconstructive duraplasty/cranioplasty. The histopathology showed osteolysis and thin walled blood vessels (occasionally cyst-like) without evidence of malignancy consistent with Gorham's disease.

Conclusion: The evaluation of a lytic lesion is a common indication for performing skeletal scintigraphy, in order to assess for the presence of primary or metastatic neoplasm. Due to the rarity of this condition, it is important for imaging doctors to consider Gorham's disease in the differential diagnosis of a lytic lesion as demonstrated in this case with multimodality imaging and histological confirmation.

P59
DERMATOMYOSITIS. UNDERLYING MALIGNANCY?

S Culleton[1]

[1]WA PET Service, Nedlands, Australia

Background: This patient presented with dermatomyositis, elevated creatinine kinase and progressive dysphagia. Dermatomyositis is an idiopathic inflammatory disease of connective tissues, manifested by skin and muscle inflammation and weakness. These symptoms may be an autoimmune response consequent to viral or bacterial infection or pregnancy, or may be a symptom of a paraneoplastic syndrome.

Aims: The clinical question to be answered was whether the patients' symptoms were caused by an underlying malignancy. 18F-Fluorodeoxyglucose (FDG) Positron Emission Tomography-Computed Tomography PET-CT has been shown to be comparable to broad conventional screening for diagnosing occult malignant disease.

Methods: The patient fasted for 6 hours and then was injected with 301 MBq of 18F-FDG. After a 60 minute uptake period the patient was scanned from vertex to feet on a Siemens Biograph 64 mCT. A low dose CT was performed for attenuation correction and anatomic localization.

Results: In this case 18F-FDG PET-CT demonstrated the likely primary, multiple metastases and a site suitable for biopsy.

Conclusion: 18F-FDG PET-CT imaging was able to answer the clinical question in a single investigation, easily tolerated by the patient.

P60
F-18 FDG UPTAKE IN AN OCULAR PROSTHESIS- A RARE FINDING ON PET/CT

N Kearney[1], S Gupta[1]

[1]Hunter New England Imaging, Nuclear Medicine & PET, Newcastle, Australia

Aim: To discuss the unusual pattern of F-18 FDG in an ocular prosthesis on a PET/CT

Method: A 78 year old female with COPD and a history of smoking was recently diagnosed with invasive adenocarcinoma in the left lower lung, she presented for an F-18 FDG PET/CT for disease staging. Imaging was performed with arms abducted from skull vertex to mid thighs with low dose CT for attenuation correction and anatomical localisation.

Results: Images demonstrated a large soft tissue density in the left lower lung laterally with intense FDG accumulation. Also identified were small hypermetabolic soft tissue densities in the right upper lung, right mid lung, medial middle lobe of the right lung, left hilar region, mediastinum, anal canal, omentum in the right anterior abdomen and left mid abdomen. Avid FDG accumulation was noted in the orbit of the left eye which is confined to an ocular prosthesis. The patient had an ocular prosthesis following a history of evisceration six years earlier.

Conclusion: F-18 FDG uptake is known to accumulate in ocular cancers, orbital cancers, metastasis to the globe from other malignancies and ocular muscles. It is unusual to demonstrate F-18 FDG uptake within a prosthetic eye on a PET scan and to date there is only one article in the literature demonstrating this phenomenon. It is thought that the uptake of radiotracer is due to the porous nature of new generation hydroxyapatite implants that enables ingrowth of host fibrovascular tissue. The fibrovascular

© 2015 The Authors
Internal Medicine Journal © 2015 Royal Australasian College of Physicians

tissue reduces the chance of the prosthesis relocating and the risk of infection developing.

P61
TWO CASES OF RHABDOMYOLYSIS: A PICTORIAL REVIEW

R Shafik-Eid[1], K Yap[1], K Taubman[1], S. Schlicht[1]

[1]St.Vincent's Hospital Department Medical Imaging, Melbourne, Australia

Background: Rhabdomyolysis is the breakdown of muscle tissue that leads to the release of muscle fiber contents into the blood. While there is a myriad of causes, the diagnosis can be difficult as it is usually occult on plain radiography and computed tomography (CT). Skeletal tracers associated with bone scans commonly accumulate within areas of muscle necrosis. Thus bone scans offer a sensitive and relatively specific diagnosis especially when combined with Single Photon Emission Computed Tomography (SPECT), clinical history and biochemistry. The pattern of uptake can be difficult to interpret and Nuclear Medicine physicians and trainees must remain cognizant of extra-skeletal patterns of uptake.

Aim: The aim of this poster is to familiarize the reader with the extra-skeletal patterns of uptake in proven cases of rhabdomyolysis.

Methods: Two cases of pathologically proven rhabdomyolysis were reviewed from the St. Vincent's Hospital Melbourne, Picture Archiving and Communication System (PACS) and key images (both planar and SPECT) provided.

Results: Rhabdomyolysis is manifest by delayed extra skeletal uptake within areas of muscle necrosis and the diagnosis is greatly aided by SPECT. Typically skeletal tracers localize within areas of calcium build up and provide a site for radionuclide deposition when combined with phosphate. Peak uptake is generally seen 24–48 hours post-injury and resolve within one week. Images to be provided (the images were not de-identified at the time of abstract)

Conclusion: Rhabdomyolysis is rare however an important diagnosis, commonly missed on conventional radiography. Skeletal tracers accumulate within areas of muscle necrosis and typically appear as tracer accumulation within affected skeletal muscle. Due to its unusual pattern of uptake Nuclear Medicine physicians should remain cognizant of the pattern of uptake on bone scan imaging.

P62
NEUROENDOCRINE (CARCINOID) TUMOUR WITH UNSUSPECTED CARDIAC METASTASIS

R Garzan[1], R Finch[2], F Khafagi[1]

[1]The Prince Charles Hospital, Brisbane, Australia
[2]Holy Spirit Northside Hospital, Brisbane, Australia

Background: Carcinoid tumours are rare neuroendocrine tumours that originate from enterochromaffin cells of the aerodigestive tract. Most carcinoid tumours express high levels of somatostatin receptors and therefore can be imaged with radiolabelled analogues of somatostatin, including indium-111 pentetreotide. This technique permits whole body scanning, which allows detection of extra-abdominal metastases.

Aims: We describe a patient with a primary ileal carcinoid tumour who was found to have an unsuspected intracardiac metastasis on pentetreotide scan, in addition to known peritoneal and hepatic metastases.

Methods: A 64 year old man presented with an 18 month history of abdominal pain and malaise. A colonoscopy suggested extrinsic compression of the ascending colon. Abdominal CT scan, In-111 Pentetreotide whole body and SPECT/CT images were performed.

Results: Abdominal CT scan showed a large right iliac fossa mesenteric mass arising from the ileum, associated with multiple peritoneal deposits and two probable hepatic metastases. Plasma chromogranin A and platelet serotonin levels were markedly elevated. On the Octreotide scan, there was intense tracer accumulation in the ileocaecal mass and multiple mesenteric foci corresponding to the peritoneal nodules seen on the CT scan, and at least three peripheral intrahepatic foci of tracer accumulation consistent with metastases. In addition, there was a focus of intense tracer accumulation in the heart which, on SPECT-CT, appeared to be located in the interventricular septum, consistent with an intramyocardial metastasis. No other extra-abdominal foci were seen. Cardiac MRI confirmed a lobulated $2.3 \times 1.4 \times 4.5$ cm mass arising from the anteroseptal myocardium. Since the intracardiac metastasis was asymptomatic, it was not resected, and he has subsequently been treated with monthly subcutaneous injections of the sustained-release octreotide long-acting somatostatin analog, Lanreotide, with electrocardiographic monitoring and serial cardiac MRI, which remained stable at 21 months of follow-up.

P63
NON-OSSIFYING FIBROMA – AN ATYPICAL PRESENTATION AND BONE SCAN APPEARANCE

R Alipour[1], K Lee[1], Q Chiam[1], H Dixson[1], A Hadjiashrafi[2], F Bonar[2]

[1]Department of Nuclear Medicine and Ultrasound, Bankstown-Lidcombe Hospital, Bankstown, Sydney, Australia
[2]Douglass Hanly Moir Pathology, Sydney, Australia

Background: Non-ossifying fibroma (NOF) is a benign lesion that occurs commonly in the diametaphysis of the long bones in the lower extremities. It is often asymptomatic and found incidentally during routine radiographic evaluation. It is considered a developmental defect with characteristic radiological stages of progression, migration and regression 'healing.' NOF shows variable degrees of uptake on bone scan, usually minimally to mildly increased during the progression and migration phase and mild hyperaemia and moderate uptake during the regression 'healing' phase.

Case Review and Results: An otherwise well 25-year-old female presented with atraumatic right distal thigh pain for 3 weeks. Her three-phase bone scan with SPECT-CT demonstrated intense focal hyperaemia in a ring like pattern on early images and markedly increased uptake on delayed images in the right distal diametaphysis of femur (most intense in the lateral cortical aspect) localising to an eccentric osteolytic lesion with an sclerotic margin on the low dose CT. There was no cortical erosion or fracture line with the lesion was noted to involve greater than 50% of the femoral diameter. The bone scan findings favoured the diagnosis of NOF complicated by micro fractures. Subsequently, a biopsy of the lesion confirmed the diagnosis of non-ossifying fibroma.

Conclusion: Bone scan was helpful in investigating this patient's lower limb pain. The biopsy was helpful to confirm the diagnosis, reassure the patient and exclude other pathologies such as fibrous dysplasia, giant cell tumour or aneurysmal bone cyst.

P64
WORK-UP OF AN INCIDENTAL SOLITARY LIVER LESION

G Rainbird[1], QL Chiam[1], R Alipour[1], C Bui[1]

[1]Bankstown Hospital, Sydney, Australia

Introduction: Solitary hepatic lesions are not uncommon and imaging aids clinical history, examination, and laboratory results to determine if it is benign or malignant and consequently appropriate management.

Clinical History: A 38 year old female on the oral contraceptive pill was referred for evaluation of a solitary solid 4.5 cm liver lesion found incidentally during an ultrasound examination for abnormal liver function test. Initially, a hepatic haemangioma was suspected and later focal nodular hyperplasia (FNH), hepatic adenoma, and an atypical haemangioma were also considerations on a 4 phase CT scan.

Findings: Three nuclear medicine scans were performed to assess the left hepatic lesion. Firstly, Tc-99m Red Blood Cell (RBC) scintigraphy demonstrated uniform hepatic uptake with no evidence of a hepatic haemangioma. Next, there was uniform hepatic uptake on a liver-spleen scan, in keeping with a benign liver lesion, possibly representing FNH or an adenoma. Lastly, a HIDA scan demonstrated focal relatively increased hepatic uptake in the region of segment 2, with the combined scan findings consistent with FNH.

Discussion: Nuclear medicine imaging of solid liver lesions has long been established. Tc-99m RBC scintigraphy has a very high positive predictive value for hepatic haemangiomas. In Tc-99m liver-spleen scans, sulphur-colloid localises within the hepatic Kupffer cells with FNH containing all 3 hepatic cell types, including Kupffer cells. Up to 70% demonstrated normal or increase radiocolloid uptake with 30% demonstrating decreased uptake.

Hepatic adenoma are classically photopaenic on the liver-spleen scan, however, about a quarter of these lesions can demonstrate radiocolloid uptake, requiring a HIDA scan for further lesion characterisation. FNH accumulates Tc-99m-HIDA while hepatic adenomas usually do not exhibit uptake on hepatobiliary imaging.

© 2015 The Authors
Internal Medicine Journal © 2015 Royal Australasian College of Physicians

Conclusion: Nuclear medicine imaging determined that the liver lesion was benign and consistent with focal nodular hyperplasia, so avoiding the need for a biopsy with only conservative management required.

P65
RARE CASE OF RICHTER'S TRANSFORMATION OF CHRONIC LYMPHOCYTIC LEUKEMIA TO HODGKIN'S LYMPHOMA DEMONSTRATED ON FDG PET

A Iravani[1], *R Mansberg*[1,2], *L Shen*[1]

[1]*Department of Nuclear Medicine and PET, Nepean Hospital, Kingswood, Australia*
[2]*University of Sydney, Sydney, Australia*

Background: Approximately 2–8% of patients with chronic lymphocytic leukemia (CLL) will transform into a more aggressive clinical entity known as Richter's transformation (RT). The most common histological transformation is to a high-grade non-Hodgkin lymphoma (NHL), with other entities rarely described, including Hodgkin lymphoma (HL) variant. Clinical features of RT are nonspecific and suggestive laboratory findings (raised lactate dehydrogenase and β-2 microglobulin) can frequently be seen in patients without RT. FDG-PET is widely used for the initial staging and restaging of HL and NHL and may therefore be used for this purpose in patients with CLL. FDG-PET can detect transformation of CLL to NHL with a high sensitivity (91%) and a high negative predictive value (97%), however rarity of Hodgkin variant precludes similar analysis. A SUVmax of at least 5 within a lymph node or extranodal site is considered strongly suggestive of RT, whereas values of less than 5 indicate a more indolent phase of CLL.

Aims: To demonstrate the role of FDG-PET in the early detection and accurate staging of a rare case of Hodgkin's variant of RT.

Methods and Results: We present a 62-year-old male with a twelve-year history of CLL with four months of constitutional symptoms and enlarging lymphadenopathy. The prior treatments include chlorambucil/prednisolone and over the last two years fludarabine/rituximab. Fine needle aspiration of the cervical lymph nodes and bone marrow was consistent with CLL, however subsequent excisional biopsy of the axillary lymph nodes revealed Hodgkin variant of RT. FDG-PET demonstrated stage IV (Ann Arbor) HL with intensely FDG avid (SUVmax 15) left axillary and multiple nodal stations on both sides of the diaphragm and extranodal involvement of the liver.

Conclusion: In this patient FDG-PET supported the clinical impression of RT and provided information required for the accurate staging.

P66
AN INCIDENTAL DIAGNOSIS OF THYROID CANCER ON A PARATHYROID STUDY

E Wright[1], *S Peters*[1], *K McNeil*[1], *D Sivaratnam*[1]

[1]*St FX Cabrini Hospital, Malvern, Australia*

Background: Parathyroid scintigraphy is used to diagnose and localise parathyroid adenomas. Adenomas are clinically suggested in the presence of increased serum calcium levels and elevated parathyroid hormone (PTH). A 54 year old woman presented to the department with elevated calcium and fluctuating PTH levels. She was otherwise well.

Aim: The following case highlights an unusual, but important, incidental finding.

Method: A parathyroid scan was performed using a low dose thyroid scan to assess thyroid shape followed by administration of 800 MBq of 99mTc-Sestamibi (MIBI). Planar images were acquired at 1 minute, 30 minutes and 3 hours post-injection with a SPECT acquired at 30 minutes and SPECT/CT at 3 hours. A neck ultrasound was organised for correlation.

Results: The parathyroid scan was consistent with an adenoma inferior to the thyroid gland. The ultrasound confirmed this conclusion. At the time of surgery a locally advanced thyroid carcinoma was found corresponding to the area of persistent MIBI uptake which was thought to represent an adenoma. The carcinoma was removed and found to be papillary carcinoma (follicular variant) with lymphatic involvement and extension into the perithyroid soft tissue. Ablative therapy with 100 mCi of 131-Iodine was performed with whole body and SPECT/CT imaging acquired 9 days post-treatment. Scintigraphic findings showed intense 131-I uptake correlating to multiple peripherally calcified lymph nodes in the supraclavicular fossa and superior mediastinum.

Conclusion: Following this incidental finding the management of this patient was significantly changed. This patient is now being monitored closely by an endocrinologist and is scheduled to have another ablative dose of 131-Iodine in the near future. This case highlights that not all incongruent MIBI uptake on parathyroid scintigraphy that persists is an adenoma. If abnormal uptake corresponds to a large structure differential diagnosis, such as cancer should also be considered.

P67
A RARE SIGHT: IMAGING NECROTISING FASCIITIS

E J Brook[1], *N N Kohler*[1], *M McCarthy*[1]

[1]*Royal Perth Hospital, Perth, Australia*

Aim: To demonstrate the usefulness of hexamethylpropyleneamine oxine (HMPAO) white cell labelling in the evaluation of osteomyelitis.

Methods: Infection imaging using HMPAO labelled white cells was performed on a 64 year old male who presented following treatment for necrotising fasciitis. Symptoms of necrotising fasciitis had subsided however swelling and tenderness remained over the left lateral malleuolus despite multiple debridement's. The patients' white blood cells were labelled with 470 MBq 99mTc HMPAO prior to injection. Delayed static images of the lower legs were acquired four hours post-injection, followed by SPECT/CT.

Results: Wide spread superficial soft tissue activity was seen extending to the left knee with focal activity at the left lateral malleoulus. The intensity and focal concentration of white cell activity over the left lower leg is consistent with the location of the skin graft, with highly intense focal activity over the left lateral malleoulus, consistent with the area of interest in regard to osteomyelitis. The SPECT/CT images confirm localisation within the boney anatomy of the left lateral malleoulus suggesting osteomyelitis.

Conclusion: HMPAO labelled white blood cells was very helpful in confirming osteomyelitis involvement at the site of concern.

P68
WIDESPREAD PERIOSTITIS DUE TO ACUTE SYPHILIS: A CASE STUDY

E. Langeluddecke[1]

[1]*Queen Elizabeth Hospital, Adelaide, Australia*

Background: A 38 year old male patient with known human immunodeficiency virus (HIV) and a recent diagnosis of active syphilis was admitted to hospital to undergo a lumber puncture to investigate suspected neurosyphilis. The patient had also been complaining for several months of ongoing shin pain. A bone scan was requested.

Aims: To present a rare bone scan finding of periosteal osteitis as a direct result of syphilis infection.

Methods: Following department protocol, after intravenous injection of 99mTc-Methyl diphosphonate (MDP) early flow and blood pool images were acquired of the lower legs, followed by delayed whole body imaging and SPECT/CT of the lower legs.

Results: The bone scan demonstrated diffuse hyperaemia in the early images and delayed widespread periosteal uptake. Given the patient's clinical history and recent testing for known active syphilis it was concluded that the patients shin pain and general body aches were a result of syphilitic periostitis. The tibia, radius and ulna, skull and clavicles all demonstrated signs of focal osteoblastic activity. Syphilis is a sexually transmitted disease caused by the bacteria spirochete *treponema pallidum*. It is characterised by three stages of disease that take affect from 10 days to 15 years (if left untreated) after exposure. In this case the infection caused pain from inflammation of the skeletal system. The patient went on to be treated with a prolonged course of intravenous benzathine penicillin.

Conclusion: Syphilis is often thought to be a rare disease of only historical significance, however in recent years incidences in occurrence in men have seen a rise in Australia. A review of the literature indicates that conventional radiographs and CT do not demonstrate the signs of syphilitic periostitis, particularly in the early stages. MRI can be effective in diagnosing syphilitic periostitis but is not able to easily assess the entire skeleton, making nuclear medicine bone scintigraphy advantageous.

© 2015 The Authors
Internal Medicine Journal © 2015 Royal Australasian College of Physicians

P69
QUALITY CONTROL OF PET RADIOPHARMACEUTICALS: PGIMER, CHANDIGARH EXPERIENCE

N Garg[1], J Shukla[2], B.R.Mittal[2]

[1]Fortis Hospital, Ludhiana, India
[2]Pgimer, Chandigarh, India

Background: PET is the medical imaging modality in which patient is injected with radiopharmaceutical. The quality control of radiopharmaceutical is an important aspect to ensure the purity, potency, product identity, biologic safety and efficacy of radiopharmaceutical.

Aim: To assess radionuclide purity, radiochemical purity, apyrogenicity and sterility of PET radiopharmaceuticals 18FDG, 13NH3 and 68Ga-DOTATATE.

Methods: The samples of 18FDG, 68Ga-DOTATATE (n = 25 each) and 13NH3 (n = 10) were randomly selected. The radionuclidic purity was assessed by half-life (t1/2) determination by recording activity after every 10 min for F-18,Ga-68 and after every 10 sec for N-13. N-13 impurity in 18FDG was assessed by recording MCA spectra of 18FDG and t1/2 of N-13. ITLC of 18FDG and 68Ga-DOTATATE was done by using acetonitrile : water (85:15) and sodium citrate as mobile phase, to assess radiochemical purity. The chemical purity was checked by gas chromatography using ethanol (4000 ppm) and acetonitrile (400 ppm) as standards. Kryptofix impurity was determined by colour chromatography using methanol: ammonium hydroxide (90:10) as mobile phase and I2 vapours as colour developer. All the samples were incubated in RCM broth at 37°C for 3–4 days to determine the sterility. Bacterial endotoxin test was performed by LAL reagents with positive and negative controls.

Result: Result of various tests performed.

Test	Method	^{18}F-FDG	^{68}Ga-DOTATATE	^{13}N-NH$_3$
pH	pH Check	4.5–8.8	4.5–8.5	4.5–8.5
Radionuclidic Purity	Half-life	105–110 minutes	68 minutes	10 minutes
	Gamma-Spetrum	Photon Energy (PE) of 0.511–1.022 keV	PE0.511–1.022 keV	PE0.511–1.022 keV
Radiochemical Purity	TLC	Rf 0.4–0.45	Rf 16–2.2	NOT APPLICABLE (NA)
Chemical Purity	Kryptofix test	Sample spot lighter than reference spot	NA	NA
Residual solvent	Ethanol	>4000 ppm	>4000 ppm	NA
	Acetonitrile	>400 ppl	NA	NA
Sterility	Standard sterility test	No bacterial growth (NBG)	NBG	NBG
Bacterial Endotoxin Test	GelClot Method	No gel formation (NGF)	NGF	NGF

Conclusion: 18FDG, 68Ga-DOTATATE and 13NH3 conformed to various quality attributes of purity; efficacy and safety in the randomized samples and are safe for patient's use.

P70
BIODISTRIBUTION OF SIRSPHERES ON 90Y-PET/CT VS. BREMSSTRAHLUNG SPECT/CT IN PATIENTS WITH LIVER CARCINOMA

W Ng[1], D Thomas[1], K Pathmaraj[1], S Lee[1], Y Kao[1], M Goodwin[1], A Scott[1]

[1]Department of Molecular Imaging and Therapy, and Department of Radiology, Austin Health, Melbourne, Australia

Background: SIR-spheres are being used more widely for treatment of liver carcinoma, and assessment of biodistribution of the radiolabelled microspheres may assist in assessing the target to non-target ratio of the treatment. SPECT/CT has been the diagnostic tool of choice to evaluate the success of SIR-Spheres administration with Bremsstrahlung imaging. Although only a very small percentage of the decay of Yttrium-90 results in pair production and detection by PET/CT, improved resolution can be obtained from PET imaging compared to SPECT.

Aim: To perform a qualitative comparison of biodistribution of ^{90}Y-labelled microspheres on ^{90}Y-PET/CT imaging versus ^{90}Y-Bremsstrahlung SPECT/CT imaging.

Methods: Twenty-five patients with end stage liver carcinoma (primary and metastatic) treated with intra-arterial hepatic infusion of ^{90}Y-SIR-spheres had post-treatment PET/CT and Bremsstrahlung SPECT/CT performed on the same day. The imaging time for both modalities was 20 minutes each. The images were reviewed by two experienced independent Nuclear Medicine Physicians to assess for biodistribution of the radiolabelled microspheres, and compared to the diagnostic contrast enhanced CT.

Results: Tumour identification and definition of targeting by radiolabelled microspheres was significantly improved on ^{90}Y-PET/CT compared to ^{90}Y-Bremsstrahlung SPECT/CT images, which corresponded to small contrast enhancing lesions on diagnostic CT. Few patients had non-target intrahepatic and extrahepatic activity, which was more confidently detected on the PET/CT than SPECT/CT, but did not have any significant impact on patient morbidity post-treatment.

Conclusion: In this cohort of patients with primary or metastatic liver carcinoma, ^{90}Y-PET/CT demonstrates superior detection of biodistribution of radiolabelled SIR-spheres compared to ^{90}Y-Bremsstrahlung SPECT/CT, improves physician confidence in diagnostic reporting, and assists with dosimetric analysis.

P71
DOSIMETRY OF ^{124}I-PEG-AVP0458 DIABODY IN PATIENTS WITH TAG-72 POSITIVE OVARIAN OR PROSTATE CANCER

SJ. Gong[1], GJ. O'Keefe[1,2], ST Lee[1,2], T Akhurst[3], FT Lee[2], I Davis[4], A Weickhardt[2,5], H Gan[2,5], K Pathmeraj[1], RJ. Hicks[3], PJ. Hudson[6], AM. Scott[1,2]

[1]Department of Molecular Imaging and Therapy, Austin Health, Melbourne, Australia
[2]Olivia Newton-John Cancer Research Institute, and La Trobe University, Melbourne, Australia
[3]Department of Cancer Imaging, Peter MacCallum Cancer Centre, Melbourne, Australia
[4]Eastern Health Clinical School, Monash University, Melbourne, Australia
[5]Ludwig Institute Oncology Unit, Austin Hospital, Melbourne, Australia
[6]Avipep Pty Ltd, and Victorian Cancer Biologics Consortium, Melbourne, Australia

Background: A phase I first-in-human clinical trial of ^{124}I-PEG-AVP0458 in patients with TAG-72 positive ovarian or prostate cancer has been carried out to determine the tumour targeting potential of PEG-AVP0458, a diabody containing the modified CC49 antibody sequences. This study aimed to elucidate the biodistribution, estimate the tracer kinetics and assess the internal radiation dose of ^{124}I-PEG-AVP0458 in the patients enrolled.

Methods: A total of 5 of 6 recruited patients had their PET/CT whole-body scans undertaken on Day 0, Day 1, Day 2 or 3, Day 4 or 5, and Day 6 or 7, following the IV administration of a single dose of ^{124}I-PEG-AVP0458 (196.99 ± 8.42 MBq). The whole-body clearance rate and uptakes in sixteen major organs and reference tumours were quantitatively assessed from the sequential images using PMOD. The internal radiation doses were derived from the ^{124}I-PEG-AVP0458 kinetic data of two patients using OLINDA 1.0 EXM.

Results: No significant differences of the effective half-life ($p = 0.97$) and biological half-life ($p = 0.89$) were observed between the 1 mg/m^2 and 10 mg/m^2 PEG-AVP0458 dose cohort groups, with mean effective half-life of 57.40 ± 4.73 hr and mean biological half-life of 136.59 ± 25.55 hr. In the three patients whose tumours were clearly evident on ^{124}I-PEG-AVP0458 PET images, there was a mean tumour AUC to serum AUC ratio of 3.33 ± 2.87, and the mean liver AUC to serum AUC ratio of 0.40 ± 0.04. The highest mean dose, 0.096 mGy/MBq, was seen in the stomach, whereas the lowest mean dose, 0.009 mGy/MBq, was seen in the brain. The ED was 0.54 mSv/MBq.

Conclusions: The estimated organ doses for ^{124}I-PEG-AVP0458 are low, and tumour : normal tissue ratios are superior to typical intact humanised

© 2015 The Authors
Internal Medicine Journal © 2015 Royal Australasian College of Physicians

IgG antibodies. These dosimetry results indicate that radioimmunotherapy with ^{124}I-PEG-AVP0458 is highly feasible and warrants clinical evaluation.

P72
THE SLACK METRIC FOR VALIDATION OF INTERNAL DOSIMETRY FOR RADIONUCLIDE THERAPY

E.McKay[1]

[1]*St. George Hospital, Sydney, Australia*

Background: Evaluation of systems for radionuclide therapy dosimetry requires a metric related to the deterministic effects and side-effects of therapy. Mean dose is insufficient, as radiobiological outcomes depend on dose distribution. Alternatively, the surviving fraction (SF) of cells in a target region is sensitive to small variations in spatial and temporal dose distribution and has a simple physical interpretation.

Aims: A metric based on SF, the Simulated Log Anticipated Cell Kill (SLACK), is developed and used to evaluate an implementation of voxel-level dosimetry.

Methods: The SLACK of a dose distribution is defined as $-\log_{10}(SF_{vol})$ with SF_{vol} the average SF over a volume of interest (VOI), calculated using the linear-quadratic dose response model with radiosensitivity 0.5 Gy^{-1} and potential sparing capacity 0.05 Gy^{-2}. The metric was calculated for a simulated radionuclide therapy dosimetry study. Tomographic projections of a cylindrical software phantom with standard hot sphere inserts were created at 5 time-points over 7 days, using parameters appropriate for Lu-177 imaging and assuming mono-exponential clearance with a 50 hour half-life. Images were reconstructed using 1024 iterations of OSEM. Time-activity curves were extracted from reconstructed volumes at the voxel level and exponential clearance curves were fitted to establish cumulated activity per voxel. VDK convolution was used to form a dose distribution, from which a dose volume histogram was extracted for each VOI. SLACK was calculated for each and plotted against iteration number

Results: Plots of calculated SLACK vs iteration number peak as noise in the reconstruction begins to dominate the decreasing bias, falling short of true SLACK.

Conclusion: The SLACK metric highlights a non-obvious weakness of a basic voxel dose calculation method. Future work will extend the application of the metric to more complex temporal distributions of dose and more realistic phantoms.

P73
A COMPARISON OF PAEDIATRIC DOSE GUIDELINES IN NUCLEAR MEDICINE

[1]*I Holmes*

[1]*Royal Brisbane and Women's Hospital, Brisbane, Australia*

Background: Dose reduction techniques in nuclear medicine are essential when imaging paediatrics. The long-term risk of radiation-induced malignancy after exposure to ionizing radiation is higher in paediatrics compared to adults, even when the same effective dose is received. The younger the child, the more sensitive their cells are to the effects of ionizing radiation. The 1990's saw a surge in literature on the effects of ionizing radiation in atomic bomb survivors, which lead to new risk estimates for the paediatric population. As a result, several dose formulas and guidelines were developed for paediatric imaging. In 2014, the European Association of Nuclear Medicine (EANM) published a Dosage Card (Version 1.2.2014), which contained weight-independent recommended doses for paediatric nuclear medicine.

Aim: To identify differences between paediatric dose guidelines used in current clinical practice at The Royal Brisbane and Women's hospital (RBWH) in comparison to recommendations from the EANM Dosage Card.

Method: Dose comparisons were made between RBWH dose guidelines and the EANM Dosage Card for patients aged 0–17 years for the following examinations; bone ^{99m}Tc-MDP, Meckel's diverticulum ^{99m}Tc-Pertechnetate, thyroid ^{99m}Tc-Pertechnetate, tumour ^{123}I-MIBG, renal ^{99m}Tc-MAG3, renal ^{99m}T-DMSA and brain ^{99m}Tc-HMPAO.

Results: For radiopharmaceuticals ^{99m}Tc-MDP, ^{99m}Tc-MAG3, ^{99m}T-DMSA and ^{99m}Tc-Pertechnetate, the EANM Dosage Card recommendations were lower than RBWH dose guidelines, resulting in reduced effective doses. For radiopharmaceuticals ^{99m}Tc-HMPAO and ^{123}I-MIBG, the EANM Dosage Card recommendations exceeded the maximum dose limit at RBWH for children over the age of 14 or greater than 50 kg, resulting in higher effective doses.

Conclusion: Overall, the EANM Dosage Card recommendations were lower than RBWH dose guidelines, resulting in reduced effective doses from examinations. The greatest variability between the two dose guidelines occurred in the smallest, youngest and most at risk patients.

P74
RADIONUCLIDE BONE SPECT-CT: LOWERING DOSE OF CT SIGNIFICANTLY REDUCES RADIATION DOSE WITHOUT IMPACTING THE IMAGE QUALITY

SK Gupta[1], *S Trethewey*[1], *B Brooker*[1], *N Rutherford*[1], *S Viswanathan*[1]

[1]*Hunter New England Health, Newcastle, Australia*

Introduction: SPECT-CT is valuable when performing bone scintigraphy as this provides both structural and functional information. CT is required for attenuation correction and anatomical localization of the lesions. For this purpose, the low-dose CT is performed but there is no consensus about the optimal CT acquisition parameters. In our department, a standard CT acquisition protocol was changed in 2013 to give lower radiation dose to the patient. In this study, we retrospectively compare the two CT protocols and analyse the effects on radiation dose as well as the image quality.

Method: Ninety nine consecutive patients [n = 51 Standard dose old CT protocol (SDOCP); n = 48 lower dose new protocol (LDNCP)] were examined. The SDOCP was 130 kvp tube voltage and reference current at 70 mAs. The LDNCP was changed to 110 kvp tube voltage and reference current at 40 mAs. The various quantitative parameters from the CT images (e.g. abdominal circumference, standard deviation of multiple areas of the CT for noise detection) were obtained. Two experienced nuclear medicine physicians reviewed the CTs as well for the resolution and noise of the CT images.

Results: The SDOCP and LDNCP groups were similar in the patient age, gender and abdominal circumference (p = NS). The calculated dose length product (DLP) of the LDNCP group (121.5 ± 39.6) was significantly lower compared to the SDOCP group patients (266.9 ± 96.9; $p < 0.0001$). I.e. the mean effective dose reduced from 4.0 mSv to 1.8 mSv. Quantitatively, the noise in the CT images were significantly less in the LDNCP images, compared to the SDOCP images despite lower dose. Visually, physicians reported better resolution and lesser noise for the soft tissue structures in the SDOCP group significantly better resolution for the LDNCP group for the bony structures.

Conclusion: The optimized new CT dose protocol significantly reduced the radiation dose to the patient and in-fact improved image quality for the assessment of the bony structures.

P75
RADIATION EXPOSURE TO THE FINGERS OF PET TECHNOLOGIST'S (PT'S) AT A MAJOR PUBLIC HOSPITAL IN MELBOURNE

S.Coleiro[1], *M. Cherk*[1], *V. Kalff*[1]

[1]*Alfred Hospital Melbourne, Melbourne, Australia*

Background: The Radiation Regulations of Victoria 2007 stipulate an annual ionizing radiation equivalent dose limit for occupational exposure of 500 mSv to any part of the hand. To ensure compliance with this dose limit a radiation monitoring program is required.

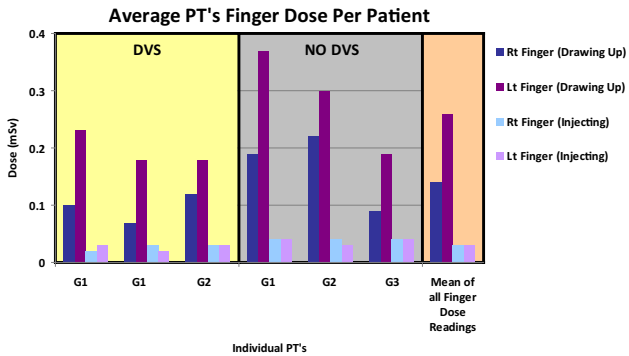
Aim: To ensure PT's are within the acceptable finger equivalent dose limit of 500 mSv/year, whilst drawing up and administering ^{18}F-Fluoro-deoxyglucose (FDG).

Methods: Six right handed PT's, Three Grade 1 (G1), Two Grade 2 (G2) and One Grade 3 (G3) wore finger TLD rings provided by Australian Radiation Services on their left and right index finger whilst drawing up and administering ^{18}F-FDG in 139 patients over a 2 month period. Radiation exposure was recorded during the drawing up phase in 83 patients in the first month and the injecting phase in 56 patients in the second month. Two G1 and one G2 PT's used a pre-calculated Dose Volume Spreadsheet (DVS) whilst drawing up doses to determine whether this also reduced finger dose.

Results: Mean index finger dose per patient across all 6 PT's during the drawing up and administration phases respectively was 0.26 mSv and 0.03 mSv

© 2015 The Authors
Internal Medicine Journal © 2015 Royal Australasian College of Physicians

on the left and 0.14 mSv and 0.03 mSv on the right. The PT with the highest dose exposure was a G1 PT who received on average 0.39 mSv to the left index finger per patient. G1 and G2 PT's that used the DVS appeared to have lower finger doses compared to G1 and G2 PT's that did not.



Conclusion: Based on each PT in our department drawing up and administering ^{18}F-FDG in 119 patients on average per year, mean left and right index finger dose respectively is estimated to be 35 mSv (range 26–51) and 20 mSv (range 14–33) per year. This is well within the 500 mSv limit.

P76
RADIATION DOSES TO STAFF IN THE EVOLVING WORLD OF NUCLEAR MEDICINE: IS RADIATION SAFETY FOR STAFF BEING MAINTAINED?

J Turner[1], L Gray[1], S Goodman[1]

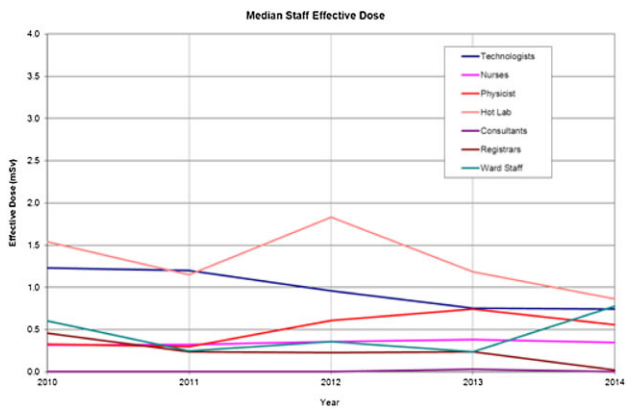
[1]The Royal Brisbane & Women's Hospital, Brisbane, Australia

Background: The utility of nuclear medicine is rapidly changing with targeted radionuclide therapies & new PET tracers being introduced. These procedures potentially result in higher levels of radiation exposure to staff during preparation, delivery and scanning. Ensuring staff do not exceed legislative occupational effective dose limits (20 mSv per year averaged over 5 years) is a pertinent issue that is closely monitored.

Aims: To assess if the shift in the utility of nuclear medicine within a large public hospital has resulted in increased radiation exposure to staff or if radiation safety practices have been implemented to ensure no increase in effective radiation dose.

Methods: A review of all staff within the department's Optically Stimulated Luminescence (OSL) dosimeter readings was conducted over a 5 year period (2010–2014). These results were broken-down to compare staffing groups (Technologists, Nurses, Physicist, Hot Lab, Consultants, Registrars & Ward Staff) with the median effective dose (mSv) for each group recorded.

Results: The results of the analysis are shown in Figure 1 below.



In the period 2010–2014 hot lab staff experienced the highest median effective dose. Overall reduction in median effective doses were identified in the technologists (1.2-0.8 mSv) and registrars (0.5-0 mSv); consultants doses remained very low (almost 0.0 mSv); nurses doses remained constant (0.3–0.4 mSv); hot lab doses overall were reduced (1.5-0.9 mSv) with a spike (1.8 mSv) in 2012; physicists & ward staff experienced an increased dose (0.3–0.6 mSv/0.6–0.8 mSv) respectively, with physicist doses now trending downwards.

Conclusion: All staffing groups are below the legislative dose limit of 20 mSv per year with radiation safety practices within the department improving in line with the changes in utility. A range of reasons are attributed to the increases in dose seen in some professional groups including new hot lab staff (2012), physicists increased hot lab workload (2011–2013) and ward staffs increased need to transport therapy/PET patients.

P77
RADIATION DOSE TO NUCLEAR MEDICINE TECHNOLOGISTS: A 9 YEAR REVIEW

N Forwood[1], D Bailey[1,2], E Bailey[1], S Macalpine[1]

[1]Royal North Shore Hospital, Sydney, Australia
[2]School of Physics, University of Sydney, Sydney, Australia

Background: Since 2006 several significant events have occurred in the nuclear medicine department at Royal North Shore Hospital, most notable the commencement of a PET service in 2010 and the move to a new hospital in 2012. During this time the department has processed 38,200 appointments and recorded >2,500 dose readings for staff.

Aim: To review the radiation dose to technologists since August 2006 and examine the influence caused by significant changes to the service.

Methods: For each employee dose reading in our records the system notes the day on which the dosimeter was given to the employee, the day on which the dosimeter was collected off the employee and the reported dose in microsieverts. The dose readings were normalized to the dosimeter wearing period by converting to an annualised dose. For each dose reading the number of bookings was determined for the period during which the dosimeter was worn. The maximum annualised dose and the average annualised dose were grouped into months by the date on which the dosimeter was handed out.

Results: Average doses have mostly been less than 2000 µSv *p.a.* which is comparable to the readings at the beginning of the survey. The initial period after introducing the PET service corresponded to an increasing radiation dose to technologists. However, after moving into a purpose-built new department and in spite of an ever-increasing PET workload, doses have not continued to rise and have even decreased slightly.

Conclusion: Detailed record keeping of occupation exposure and department workload has demonstrated that the radiation exposure of nuclear medicine technologists in our department has remained reasonably constant despite an increasing workload.

P78
ARE VENTILATION PERFUSION SCANS MORE COMMON ON FRIDAYS?

SL Vi An[1], S Singh[1], M Patel[1], L Xu[1], KK Yap[1], K Taubman[1], S Schlicht[1]

[1]Medical Imaging Department, St Vincent's Hospital, Melbourne, Australia.

Background: Ventilation perfusion scans are commonly used to evaluate for the presence of pulmonary embolic disease. Throughout nuclear medicine departments, folklore exists that these studies commonly occur on Fridays for a variety of reasons.

Aims: We aim to prove that ventilation perfusion scans are more common on Fridays.

Methods: By retrospectively assessing the PACS database, for VQ scans performed each day in absolute numbers and as a proportion of nuclear medicine studies for years from 2003 to 2013 inclusively.

Results: In the past, ventilation perfusion studies were more common as a proportion on Fridays. In 2003, ventilation perfusion imaging comprised of over 25% of the studies performed on a Friday compared to midweek where they comprised of just over 16% of studies. However in recent years this

© 2015 The Authors
Internal Medicine Journal © 2015 Royal Australasian College of Physicians

difference is largely disappeared with VQs comprising 10.9% of nuclear medicine studies on Friday in 2013.

Conclusion: In our institution, VQ scans in the past (2003/2004) were more common on Fridays, though these findings are not as apparent in recent years, presumably due to drop in absolute numbers of VQ studies and the widespread acceptance of alternate imaging techniques which have become more readily available and accessible after hours.

P79
GMP PRACTICES IN A HOSPITAL RADIOPHARMACY

D Scott[1]

[1]*Royal Brisbane and Women's Hospital, Brisbane, Australia*

Background: Facilities manufacturing products under Good Manufacturing Practices (GMP) are required to have quality systems in place to ensure that the manufacturing environment, processes and operators comply to conditions such that the product will meet industry and regulatory specifications.

Aim: This presentation will summarise the quality systems used in the hotlab at the RBWH Department of Nuclear medicine and Queensland PET services.

Method: Quality systems in place include, but are not limited to, environmental monitoring, cleaning and sanitisation, quality control, assurance and release, equipment and operator validations and documentation.

Conclusion: These systems ensure that the products manufactured at the facility meet regulatory specifications for sterile injectables and provides confidence in patient safety and affording quality health care.

P80
PATIENT FACTORS AFFECTING FLUORODEOXYGLUCOSE (FDG) SCAN CANCELLATIONS AND MINIMISATION STRATEGIES TO PREVENT FUTURE OCCURRENCES

S Sam[1], *E Stoakes*[1], *V Lord*[1], *P Lin*[1]

[1]*Nuclear Medicine & PET Department, Liverpool Hospital, Liverpool, Australia*

Background: FDG is the predominant tracer for positron emission tomography (PET) at Liverpool Hospital. As the tracer has a relatively short half-life and supply of the isotope is dependent on patient weight as well as camera availability, unplanned events can have a detrimental impact on service delivery as well as efficient use of the PET/CT scanner. Patients are always given standard booking preparation including specific diabetic instructions.

Aim: The aim of this review was to determine the causes of patient cancellation and to implement any changes to bookings in order to minimise the chances of future cancellations.

Methods: A retrospective review of patient data from February 2014 to November 2014 was undertaken. Daily worksheets were reviewed and correlated with the cancellation reason on the hospital radiology information system (RIS). Cancellation reasons were divided into the categories of patient condition, blood sugar problems, transport issues, patient preparation, team cancellation and patient refusal. The categories were further divided into whether the patients were inpatients or outpatients.

Results: During the period of review, there were 88/2542 cancellations. 60/88 were outpatients and 28/88 were inpatients. 17 cancellations (21%) were due to the patient having an issue with their blood sugar levels (BSL), all of which had known diabetes. 13 cancellations (16%) were due to a change in the patient's condition. 25 cancellations (31%) were due to the patient failing to attend (FTA) and 13 cancellations (16%) were due to a patient preparation issue.

Conclusion: A patient's deteriorating condition is not predictable or preventable. It is hoped however with the future upgraded technology, SMS alerts will improve the number of patients that FTA and patients who did not prepare properly for their appointments which made up 47% of cancelled studies.

P81
TOOLS & STRATEGIES FOR IMPROVING THE QUALITY OF CLINICAL PLACEMENTS FOR NUCLEAR MEDICINE STUDENTS

J Turner[1]

[1]*The Royal Brisbane & Women's Hospital, Brisbane, Australia*

Background: Providing quality clinical placements for nuclear medicine students is crucial to the future development of the profession. The clinical setting for all allied health professions can be a challenging environment to teach within, combine radiation & the complexities increase further. There are very few nuclear medicine specific tools or strategic publications available for clinical staff regarding providing quality clinical placements.

Aims: To clearly identify & describe a series of tools & strategies that supervisors can use within the clinical environment to improve the quality of nuclear medicine student clinical placements. These tools will empower clinical supervisors & promote improvement for future nuclear medicine students.

Methods: Collated a range of clinical tools & strategies currently being used by the State-wide group of nuclear medicine departments within Queensland Health, as well as investigated any methods being used in other local allied health disciplines. An assessment & subsequent summary of the key elements to implementing the tools & strategies was performed, with practical examples specific to nuclear medicine clinical placements provided.

Results: There are several tools & strategies currently available to nuclear medicine supervisors which are designed to improve the quality of clinical placements & are summarised in Table 1 below.

Strategy/Tool	Key Elements to Implementation
Request Lotto	A series of de-identified request forms with structured questions
	A large range of procedures should be captured
Interesting Cases Database	A catalogue of interesting cases (PACS, excel spreadsheet, PowerPoint presentation)
	Must be updated by all staff regularly & should include normal + abnormal scan appearances
Theoretical Competency Assessment	A series of set theoretical questions given to all students completing specific competencies
	The same questions are provided to all students before the assessment
	The same answers given to all supervisors
	Encourages the vital link between practical & theory components
Simulation Role Play	Involves practicing clinical tasks & skills away from the immediate pressure of clinical patients or timeframes
	Clear roles need to be set between the supervisor & the student with roles changed to encourage perspective
	Use all equipment required where possible
Five-Minute Preceptor Model	Uses predefined scenarios or scenarios as they are encountered by the student in clinical practice
	Give the student time assess the scenario
	Involve patients where ever possible
	Improves critical thinking
	***Follow this structure*:**
	What do you think we should do now?
	What led you to that conclusion?
	Many times when . . ..
	You did an excellent job at . . ...
	Next time this happens try . . ...
Reflective Practice	Involves students reflecting on their own performance & identifying areas of improvement after an event or assessment
	Enhances critical thinking
	Promotes transfer of knowledge to similar situations
Student Based Goals	Goals developed by the student independent of their university objectives
	Encourages focus on the 'big picture' not just assessments
	Give the supervisor insight into areas of interest & thus a tailored teaching approach
Student Led Days	Students take ownership for the entire scanning day or segments of the day
	Students plan the day/element independently
	Supervisor available at all times to assist
	Should be tailored based on the students level of experience/confidence

© 2015 The Authors
Internal Medicine Journal © 2015 Royal Australasian College of Physicians

Conclusion: There are many tools & strategies available to supervisors to help improve the quality of nuclear medicine student placements. Many of these tools & strategies involve little preparation & small amounts of time. With forward planning & understanding of some key principles these tools & strategies could be easily adapted to suit any nuclear medicine department. Sharing of these resources in the future between clinical centres will encourage diversity & enhance the overall experience for students undertaking clinical placements Australia-wide.

P82
NEW KIDS ON THE BLOCK

S. Scortechini[1]

[1]*Royal Brisbane and Women's Hospital, Brisbane, Australia*

Background: After many years of planning and construction, the Lady Cilento Children's Hospital (LCCH) opened on Saturday, 29 November 2014 in South Brisbane following the closure and subsequent amalgamation of the Royal Children's Hospital (RCH) and Matar Children's Hospital (MCH). Until now, majority of the Nuclear Medicine paediatric service had been provisioned by Royal Brisbane and Women's Hospital (RBWH) Department of Nuclear Medicine and Specialised PET Services Queensland. Now for the first time in Queensland there is a dedicated paediatric Nuclear Medicine and Medical Imaging service. Due to a historical partnership and valuable staff experience in providing paediatric care, a core multidisciplinary group from RBWH Nuclear Medicine was engaged by Children's Health Queensland (CHQ) from the very beginning to assist with design, planning and potential service delivery of the paediatric Nuclear Medicine service. Six months prior to opening, a Nuclear Medicine Scientist from the RBWH Nuclear Medicine was appointed to the project to assist with final stages of planning, working closely with Medical Imaging from RCH and MCH as well as the Information and Communications Technology (ICT) team.

Aim: To highlight key areas for consideration when undertaking a new service implementation whilst meeting the organisational objective of family centred care.

Method: A six month secondment was undertaken by a Nuclear Medicine Scientist who worked in conjunction with ICT and Medical Imaging as part of a multi-disciplinary commissioning team to liaise with builders, CHQ project team, interstate and international vendors as well as the various governing bodies to ensure licencing, service level agreements, policies and procedures were all in place to guarantee an operational Nuclear Medicine service for day one whilst keeping with CHQ commitment to providing family-centred care model.

Results: An operational Nuclear Medicine service was available on opening day with clinical scanning commencing soon after in a family focused environment.

Conclusion: Concentrating on the important key areas whilst working in consultation with ICT and Medical Imaging as part of a multidisciplinary team, enabled Nuclear Medicine to provide a specialised family centred care that was operational and capable of clinical service delivery on opening day.

© 2015 The Authors
Internal Medicine Journal © 2015 Royal Australasian College of Physicians